

# Fast and Accurate Variational Inference for Models with Many Latent Variables

Rubén Loaiza-Maya, Michael Stanley Smith, David J. Nott & Peter J. Danaher

May 18, 2020

Rubén Loaiza-Maya is a Post-doctoral Fellow at the Department of Econometrics and Business Statistics, Monash University; Michael Stanley Smith is Chair of Management (Econometrics) at Melbourne Business School, University of Melbourne; David J. Nott is Associate Professor of Statistics, National University of Singapore; and Peter J. Danaher is Professor of Marketing and Econometrics, Monash University. Correspondence should be directed to Michael Smith at `mike.smith@mbs.edu`.

arXiv:2005.07430v1 [stat.ME] 15 May 2020

# Fast and Accurate Variational Inference for Models with Many Latent Variables

## Abstract

Models with a large number of latent variables are often used to fully utilize the information in big or complex data. However, they can be difficult to estimate using standard approaches, and variational inference methods are a popular alternative. Key to the success of these is the selection of an approximation to the target density that is accurate, tractable and fast to calibrate using optimization methods. Mean field or structured Gaussian approximations are common, but these can be inaccurate and slow to calibrate when there are many latent variables. Instead, we propose a family of tractable variational approximations that are more accurate and faster to calibrate for this case. The approximation is a parsimonious copula model for the parameter posterior, combined with the exact conditional posterior of the latent variables. We derive a simplified expression for the re-parameterization gradient of the variational lower bound, which is the main ingredient of efficient optimization algorithms used to implement variational estimation. We illustrate using two substantive econometric examples. The first is a nonlinear state space model for U.S. inflation. The second is a random coefficients tobit model applied to a rich marketing dataset with one million sales observations from a panel of 10,000 individuals. In both cases, we show that our approximating family is faster to calibrate than either mean field or structured Gaussian approximations, and that the gains in posterior estimation accuracy are considerable.

**Key Words:** Copula Variational Approximation; Nonlinear State Space Models; Large Marketing Panels; Stochastic Gradient Ascent; Variational Bayes.

# 1 Introduction

Models with large numbers of latent variables<sup>1</sup> are increasingly popular for capturing nuances in large or complex datasets. Examples include topic models (Hoffman et al., 2013), state space models (Durbin and Koopman, 2012), choice models (Train, 2009) and mixed models (Molenberghs and Verbeke, 2006, Gelman and Hill, 2006), among many others. In some cases it is possible to integrate out the latent variables analytically or numerically, although frequently it is not. Instead, Bayesian estimation usually proceeds by considering the joint posterior distribution of the model parameters and latent variables, often called an ‘augmented posterior’. Conventional Markov chain Monte Carlo (MCMC) methods for evaluating the augmented posterior are computationally burdensome, and optimization-based variational inference (Blei et al., 2017, Ormerod and Wand, 2010) is a scalable alternative. However, existing variational methods make strong independence or other parametric assumptions which often result in a poor approximation to the augmented posterior. In this paper we suggest a general variational inference method which provides a more accurate approximation to the augmented posterior, while being scalable to the case where there are a large numbers of latent variables and global model parameters.

Key to effective variational inference (also called ‘variational Bayes’) is the selection of a suitable variational approximation (VA). We suggest a VA which uses a copula model defined through a parametric transformation (Smith et al., 2020) for the global model parameters, along with the exact conditional posterior distribution for the latent variables. We show that the approximation is tractable, and derive a method for estimating the re-parameterization gradient of the variational lower bound (Kingma and Welling, 2014, Rezende et al., 2014), which is the main input to efficient stochastic gradient ascent (SGA) methods widely used for calibrating VAs (Bottou, 2010, Paisley et al., 2012, Nott et al., 2012, Hoffman et al., 2013, Salimans et al., 2013, Ranganath et al., 2014). Importantly, our method does not require evaluation of the conditional posterior density of the latent variables, or its derivative, which are usually unavailable. Instead, only a draw from the conditional posterior

---

<sup>1</sup>In the machine learning literature latent variables are sometimes called ‘local variables’ and model parameters are sometimes called ‘global variables’; for example, see Hoffman et al. (2013).

(either exactly or approximately) is needed, which is typically straightforward using a variety of well-explored Monte Carlo methods for most models, including sub-sampling approaches suitable for very large numbers of latent variables (Quiroz et al., 2019).

In some applications poor parameter uncertainty quantification may not harm predictive inference (Wang and Blei, 2019). However, this is not the case for many latent variable models, including the two econometric applications considered here. Although marginal posterior distributions of global model parameters are often well approximated as Gaussian for large datasets (Titsias and Lázaro-Gredilla, 2014, Ong et al., 2018, Archer et al., 2015, Kucukelbir et al., 2017), observation-specific latent variables about which there is little information may exhibit highly non-Gaussian marginal posteriors. Furthermore, when the number of observation-specific latent variables grows with the sample size, poor uncertainty quantification for the latent variables can cause poor inference for the global model parameters, including inaccurate point estimates. A review of the existing literature on variational inference for complex latent variable models is given later in Section 2.4.

To illustrate the advantages of our approach we employ it to estimate two econometric models. The first is an unobserved component stochastic volatility (UCSV) model for monthly U.S. inflation (Stock and Watson, 2007, Chan, 2013). This is a nonlinear state space model, where the first two moments of inflation are latent states. Mean field approximations are known to be very poor for state space models (Wang and Titterton, 2004), and Gaussian VAs with parsimonious structured covariance matrices are the most popular choice (Quiroz et al., 2018). Because this is a setting where exact posterior inference can be computed using existing MCMC methods, the accuracy of our VA can be assessed. We find that our method provides an approximation that is close to the true posterior and is much more accurate than a structured Gaussian VA.

The second example is a random coefficient tobit (i.e. censored regression) model applied to a large disaggregate marketing database originating from (Danaher et al., 2020). Random coefficient models are widely used in marketing to capture consumer-level heterogeneity (Allenby and Rossi, 1998) and in these models estimates of the random coefficients are central as they are used to tailor advertising and promotions at the consumer level (Rossi et al., 1996, Danaher et al., 2015).

While MCMC methods are often used to estimate these models, they are increasingly impractical to employ with contemporary large datasets, so that recent marketing studies employ variational inference instead (Ansari et al., 2018, Danaher et al., 2020). In their original study Danaher et al. (2020) employ a structured Gaussian VA, and we show that this is less accurate than our proposed VA using the exact posterior for a sub-sample of the data. Exact posterior evaluation is not viable for the full dataset of one million observations and 100,000 random coefficient values, yet we show that our approach is readily applied to this case and more effective than the Gaussian VA. Interestingly, when the trade-off between per-iteration computation time and speed of convergence in the variational optimization is considered, our proposed approximations can be calibrated accurately in 20% to 50% of the time taken by the Gaussian alternatives in these examples.

In the next section we provide an introduction to variational approximation methods, introduce our new methodology, and discuss related existing variational inference methods. Section 3 applies our approach to the UCSV model for U.S. inflation, and Section 4 to the mixed effects tobit model for the large marketing dataset. Section 5 gives a concluding discussion, including some suggestions for further extensions of the method. Appendices A and B provide a proof and implementation details for our method, while a Web Appendix provides additional details and results for the two applications.

## 2 Methodology

In this section, we first provide a short overview of variational inference. Our new family of variational approximations (VAs) for models with latent variables is then outlined, along with how they can be used to provide efficient variational inference.

### 2.1 Variational Inference

We consider Bayesian inference with data  $\mathbf{y}$  having density  $p(\mathbf{y}|\boldsymbol{\psi})$ , where in our paper,  $\boldsymbol{\psi}$  contains the model parameters augmented with a potentially large number of latent variables. Assuming a prior density  $p(\boldsymbol{\psi})$ , Bayesian inference is based on the density  $p(\boldsymbol{\psi}|\mathbf{y}) \propto p(\boldsymbol{\psi})p(\mathbf{y}|\boldsymbol{\psi})$ , which in our paper is the augmented posterior. We will consider variational inference methods, in which a member  $q_\lambda(\boldsymbol{\psi})$  of some parametric family of densities is used to approximate the target  $p(\boldsymbol{\psi}|\mathbf{y})$ , where

$\boldsymbol{\lambda} \in \Lambda$  is a vector of variational parameters. Approximate Bayesian inference is then formulated as an optimization problem, where a measure of divergence between  $q_{\boldsymbol{\lambda}}(\boldsymbol{\psi})$  and  $p(\boldsymbol{\psi}|\mathbf{y})$  is minimized with respect to  $\boldsymbol{\lambda}$ . The Kullback-Leibler divergence

$$\text{KL}(q_{\boldsymbol{\lambda}}(\boldsymbol{\psi})||p(\boldsymbol{\psi}|\mathbf{y})) = \int \log \frac{q_{\boldsymbol{\lambda}}(\boldsymbol{\psi})}{p(\boldsymbol{\psi}|\mathbf{y})} q_{\boldsymbol{\lambda}}(\boldsymbol{\psi}) d\boldsymbol{\psi},$$

is typically used, and we employ it here. If  $p(\mathbf{y}) = \int p(\boldsymbol{\psi})p(\mathbf{y}|\boldsymbol{\psi})d\boldsymbol{\psi}$  denotes the marginal likelihood, then it is easily shown (see, for example, Ormerod and Wand (2010)) that

$$\begin{aligned} \text{KL}(q_{\boldsymbol{\lambda}}(\boldsymbol{\psi})||p(\boldsymbol{\psi}|\mathbf{y})) &= \log p(\mathbf{y}) - \int \log \frac{p(\boldsymbol{\psi})p(\mathbf{y}|\boldsymbol{\psi})}{q_{\boldsymbol{\lambda}}(\boldsymbol{\psi})} q_{\boldsymbol{\lambda}}(\boldsymbol{\psi}) d\boldsymbol{\psi} \\ &= \log p(\mathbf{y}) - \mathcal{L}(\boldsymbol{\lambda}), \end{aligned} \tag{1}$$

where  $\mathcal{L}(\boldsymbol{\lambda})$  is called the variational lower bound.<sup>2</sup> Because  $\log p(\mathbf{y})$  does not depend on  $\boldsymbol{\lambda}$ , minimization of the Kullback-Leibler divergence above with respect to  $\boldsymbol{\lambda}$  is equivalent to maximizing the variational lower bound  $\mathcal{L}(\boldsymbol{\lambda})$ .

The lower bound takes the form of an intractable integral, so it seems challenging to optimize. However, notice that from (1) it can be written as an expectation with respect to  $q_{\boldsymbol{\lambda}}$  as

$$\mathcal{L}(\boldsymbol{\lambda}) = E_{q_{\boldsymbol{\lambda}}} [\log g(\boldsymbol{\psi}) - \log q_{\boldsymbol{\lambda}}(\boldsymbol{\psi})], \tag{2}$$

where  $g(\boldsymbol{\psi}) = p(\boldsymbol{\psi})p(\mathbf{y}|\boldsymbol{\psi})$ . This expression allows easy application of stochastic gradient ascent (SGA) methods (Robbins and Monro, 1951, Bottou, 2010). In SGA we start from an initial value  $\boldsymbol{\lambda}^{(0)}$  for  $\boldsymbol{\lambda}$  and update it recursively as

$$\boldsymbol{\lambda}^{(i+1)} = \boldsymbol{\lambda}^{(i)} + \boldsymbol{\rho}_i \circ \widehat{\nabla_{\boldsymbol{\lambda}} \mathcal{L}(\boldsymbol{\lambda}^{(i)})}, \text{ for } i = 1, 2, \dots,$$

where  $\boldsymbol{\rho}_i = (\rho_{i1}, \dots, \rho_{im})^{\top}$  is a vector of step sizes, ‘ $\circ$ ’ denotes the element-wise product of two vectors, and  $\widehat{\nabla_{\boldsymbol{\lambda}} \mathcal{L}(\boldsymbol{\lambda}^{(i)})}$  is an unbiased estimate of the gradient of  $\mathcal{L}(\boldsymbol{\lambda})$  at  $\boldsymbol{\lambda} = \boldsymbol{\lambda}^{(i)}$ . For appropriate step size choices this will converge to a local optimum of  $\mathcal{L}(\boldsymbol{\lambda})$ . Adaptive step size choices are often used in practice, and we use the ADADELTA method of Zeiler (2012).

To implement SGA, unbiased estimates of the gradient of the lower bound are the key requirement. These can be obtained directly by differentiating (2) with respect to  $\boldsymbol{\lambda}$ , and evaluating the expectation

---

<sup>2</sup>This is also widely called the Evidence Lower Bound (ELBO).

in a Monte Carlo fashion by simulating from  $q_\lambda$ . However, variance reduction methods for the gradient estimation are often also important for fast convergence and stability. One of the most useful is the ‘re-parametrization trick’ (Kingma and Welling, 2014, Rezende et al., 2014). In this approach, it is assumed that an iterate  $\boldsymbol{\psi}$  can be generated from  $q_\lambda$  by first drawing  $\boldsymbol{\varepsilon}$  from a density  $f_\varepsilon$  which does not depend on  $\boldsymbol{\lambda}$ , and then transforming  $\boldsymbol{\varepsilon}$  by a deterministic function  $\boldsymbol{\psi} = h(\boldsymbol{\varepsilon}, \boldsymbol{\lambda})$  of  $\boldsymbol{\varepsilon}$  and  $\boldsymbol{\lambda}$ . From (2), the lower bound can be written as the following expectation with respect to  $f_\varepsilon$ :

$$\mathcal{L}(\boldsymbol{\lambda}) = E_{f_\varepsilon} [\log g(h(\boldsymbol{\varepsilon}, \boldsymbol{\lambda})) - \log q_\lambda(h(\boldsymbol{\varepsilon}, \boldsymbol{\lambda}))] . \quad (3)$$

Differentiating under the integral sign in (3) gives the ‘re-parameterization gradient’

$$\nabla_\lambda \mathcal{L}(\boldsymbol{\lambda}) = E_{f_\varepsilon} [\nabla_\lambda \{\log g(h(\boldsymbol{\varepsilon}, \boldsymbol{\lambda})) - \log q_\lambda(h(\boldsymbol{\varepsilon}, \boldsymbol{\lambda}))\}] , \quad (4)$$

and approximating the expectation at (4) by Monte Carlo using one or more random draws from  $f_\varepsilon$  gives an unbiased estimate of  $\nabla_\lambda \mathcal{L}(\boldsymbol{\lambda})$ . An intuitive reason for the success of the re-parameterization trick is that it allows gradient information from the log-posterior to be used, by moving the variational parameters inside  $g(\boldsymbol{\psi})$  in (3). For a well-chosen VA, only one draw from  $f_\varepsilon$  is typically sufficient for the SGA to converge reliably. Xu et al. (2018) show how the trick reduces the variance of the gradient estimates when  $q_\lambda$  is a Gaussian with diagonal covariance matrix (i.e. a mean field Gaussian approximation). We employ the re-parameterization trick throughout, and specify a function  $h$  in Sections 2.2 and 2.3.

## 2.2 Variational approximations for models with latent variables

In this paper we consider the case where  $\boldsymbol{\psi}^\top = (\boldsymbol{\theta}^\top, \boldsymbol{z}^\top)$  is a parameter vector  $\boldsymbol{\theta}$  augmented with additional continuous-valued latent variables  $\boldsymbol{z}$ . Examples include state space models where  $\boldsymbol{z}$  are latent states (Durbin and Koopman, 2012), discrete choice models where  $\boldsymbol{z}$  are latent utilities (Train, 2009) and mixed models where  $\boldsymbol{z}$  are the realizations of random coefficients (Molenberghs and Verbeke, 2006, Gelman and Hill, 2006). The prior is given by  $p(\boldsymbol{\psi}) = p(\boldsymbol{z}|\boldsymbol{\theta})p(\boldsymbol{\theta})$ , and we approximate the augmented posterior density  $p(\boldsymbol{\psi}|\boldsymbol{y}) = p(\boldsymbol{\theta}, \boldsymbol{z}|\boldsymbol{y}) \propto p(\boldsymbol{y}|\boldsymbol{\theta}, \boldsymbol{z})p(\boldsymbol{z}|\boldsymbol{\theta})p(\boldsymbol{\theta}) \equiv g(\boldsymbol{\theta}, \boldsymbol{z})$  with VAs of the form

$$q_\lambda(\boldsymbol{\theta}, \boldsymbol{z}) = p(\boldsymbol{z}|\boldsymbol{y}, \boldsymbol{\theta}) q_\lambda^0(\boldsymbol{\theta}) . \quad (5)$$

As we discuss below, it must be feasible to generate directly or approximately from  $p(\mathbf{z}|\mathbf{y}, \boldsymbol{\theta})$ , although it is unnecessary to evaluate this density or its derivatives. The density  $q_\lambda^0$  is chosen to be analytically tractable and from which it is convenient to sample, and we outline a choice that can be applied generally in Section 2.3. Calibration of  $q_\lambda$  at (5) has the potential of being much more efficient than exact sampling using MCMC, because at each VB step we draw the vector  $\boldsymbol{\theta}$  jointly from  $q_\lambda^0$ , and do not require blocking of  $\boldsymbol{\theta}$  or Metropolis-Hastings steps as in many MCMC schemes.

A key reason why (5) is an attractive choice can be seen by evaluating the lower bound (2) as

$$\begin{aligned} \mathcal{L}(\boldsymbol{\lambda}) &= E_{q_\lambda} [\log g(\boldsymbol{\theta}, \mathbf{z}) - \log q_\lambda(\boldsymbol{\theta}, \mathbf{z})] \\ &= E_{q_\lambda} [\log p(\mathbf{y}|\mathbf{z}, \boldsymbol{\theta}) + \log p(\mathbf{z}|\boldsymbol{\theta}) + \log p(\boldsymbol{\theta}) - \log q_\lambda^0(\boldsymbol{\theta}) - \log p(\mathbf{z}|\mathbf{y}, \boldsymbol{\theta})] . \end{aligned} \quad (6)$$

From Bayes theorem  $p(\mathbf{z}|\mathbf{y}, \boldsymbol{\theta}) = p(\mathbf{y}|\mathbf{z}, \boldsymbol{\theta})p(\mathbf{z}|\boldsymbol{\theta})/p(\mathbf{y}|\boldsymbol{\theta})$ , substituting this into (6) and cancelling terms, results in the expression

$$\mathcal{L}(\boldsymbol{\lambda}) = E_{q_\lambda} [\log p(\mathbf{y}|\boldsymbol{\theta}) + \log p(\boldsymbol{\theta}) - \log q_\lambda^0(\boldsymbol{\theta})] = \mathcal{L}^0(\boldsymbol{\lambda}) . \quad (7)$$

Here,  $\mathcal{L}^0(\boldsymbol{\lambda})$  is the variational lower bound arising from approximating the posterior  $p(\boldsymbol{\theta}|\mathbf{y})$  directly by the VA  $q_\lambda^0$ . Thus, maximizing  $\mathcal{L}(\boldsymbol{\lambda})$  using SGA methods is equivalent to maximizing  $\mathcal{L}^0(\boldsymbol{\lambda})$  for the posterior of  $\boldsymbol{\theta}$  with  $\mathbf{z}$  marginalized out exactly, yet avoids the computation of the (often intractable) density  $p(\boldsymbol{\theta}|\mathbf{y})$  and its derivative.

A second major advantage of the VA at (5) is that the gradient of the lower bound at (4) has a simplified expression when using the re-parameterization trick, as summarized in the theorem below.

**Theorem 1** (Re-parameterization Gradient). *Let  $\boldsymbol{\varepsilon} = ((\boldsymbol{\varepsilon}^0)^\top, \mathbf{z}^\top)^\top$  have the product density  $f_\varepsilon(\boldsymbol{\varepsilon}) = f_{\varepsilon^0}(\boldsymbol{\varepsilon}^0)p(\mathbf{z}|h^0(\boldsymbol{\varepsilon}^0, \boldsymbol{\lambda}), \mathbf{y})$ , where  $f_{\varepsilon^0}$  does not depend on  $\boldsymbol{\lambda}$ , such that there exists a (vector-valued) transformation  $h$  from  $\boldsymbol{\varepsilon}$  to the augmented parameter space given by  $\boldsymbol{\psi} = h(\boldsymbol{\varepsilon}, \boldsymbol{\lambda}) = (h^0(\boldsymbol{\varepsilon}^0, \boldsymbol{\lambda})^\top, \mathbf{z}^\top)^\top$ , with  $\boldsymbol{\theta} = h^0(\boldsymbol{\varepsilon}^0, \boldsymbol{\lambda})$ . Then the re-parametrization gradient used to implement SGA is*

$$\nabla_\lambda \mathcal{L}(\boldsymbol{\lambda}) = E_{f_\varepsilon} \left( \frac{\partial \boldsymbol{\theta}^\top}{\partial \boldsymbol{\lambda}} [\nabla_\theta \log g(\boldsymbol{\theta}, \mathbf{z}) - \nabla_\theta \log q_\lambda^0(\boldsymbol{\theta})] \right) \quad (8)$$

*Proof.* See Appendix A. □

In (8), derivatives with respect to  $\log p(\mathbf{z}|\boldsymbol{\theta}, \mathbf{y})$  are not needed, greatly simplifying its calculation.



Instead, only a draw from the conditional posterior of the latent variables  $p(\mathbf{z}|\boldsymbol{\theta}, \mathbf{y})$  is required to evaluate the re-parameterization gradient. There is a large literature on drawing either exactly, or approximately, from this distribution for a wide range of latent variable models using filtering, particle, MCMC or other methods. In the two applications considered here, we use either a single, or a small number, of sweeps from a Gibbs sampler initialized at the draw from the previous SGA step. This proves effective and simple to implement. Some further remarks about the possibility of an exact implementation using newly-developed MCMC coupling approaches (Jacob et al., 2020) are given in Section 5.

### 2.3 Copula variational approximation

The final ingredient of our VA at (5) is  $q_\lambda^0(\boldsymbol{\theta})$ , along with a matching re-parameterization transformation  $\boldsymbol{\theta} = h^0(\boldsymbol{\varepsilon}^0, \boldsymbol{\lambda})$ . An advantage is that any existing variational family can be used for  $q_\lambda^0(\boldsymbol{\theta})$ . Popular candidates include mean field Gaussian or elliptical distribution approximations, although we stress this is not the same as employing such approximations for the entire augmented posterior  $p(\boldsymbol{\theta}, \mathbf{z}|\mathbf{y})$ . Here, we follow Smith et al. (2020) and use a copula-based approximation constructed using an element-wise transformation<sup>3</sup> of  $\boldsymbol{\theta} = (\theta_1, \dots, \theta_m)^\top$ . These authors show that this is a more accurate VA than either Gaussian or skew-normal distributions, but at little or no increase in computational cost. We provide an outline here, but refer to the work of these authors for details.

Let  $t_\gamma$  be a family of one-to-one transformations onto the real line with parameter vector  $\boldsymbol{\gamma}$ . To construct  $q_\lambda^0$ , we transform each parameter as  $\vartheta_i = t_{\gamma_i}(\theta_i)$  and adopt a known distribution function  $F(\boldsymbol{\vartheta}; \boldsymbol{\pi})$ , with vector of parameters  $\boldsymbol{\pi}$ , for  $\boldsymbol{\vartheta} = (\vartheta_1, \dots, \vartheta_m)^\top$ . For example, if  $F$  is a Gaussian distribution function, then  $\boldsymbol{\pi} = (\boldsymbol{\mu}_\vartheta^\top, \text{vech}(\boldsymbol{\Sigma}_\vartheta)^\top)^\top$ , where  $\boldsymbol{\mu}_\vartheta$  and  $\boldsymbol{\Sigma}_\vartheta$  are the mean and covariance matrix, and ‘vech’ is the half-vectorization operator. If  $p(\boldsymbol{\vartheta}; \boldsymbol{\pi}) = \frac{\partial^m}{\partial \vartheta_1 \dots \partial \vartheta_m} F(\boldsymbol{\vartheta}; \boldsymbol{\pi})$ , then the density of the approximation can be recovered by computing the Jacobian of the element-wise transformation from  $\boldsymbol{\theta}$  to  $\boldsymbol{\vartheta}$ , so that

$$q_\lambda^0(\boldsymbol{\theta}) = p(\boldsymbol{\vartheta}; \boldsymbol{\pi}) \prod_{i=1}^m t'_{\gamma_i}(\theta_i), \quad (9)$$

where the variational parameters are  $\boldsymbol{\lambda}^\top = (\boldsymbol{\gamma}_1^\top, \dots, \boldsymbol{\gamma}_m^\top, \boldsymbol{\pi}^\top)$  and  $t'_{\gamma_i}(\theta_i) = \frac{d\vartheta_i}{d\theta_i}$ . Moreover, if  $F$

---

<sup>3</sup>This is not to be confused with the transformation  $h^0$  associated with the re-parameterization trick.

has known marginal distribution functions  $F_i(\vartheta_i; \boldsymbol{\pi}_i)$  and densities  $p_i(\vartheta_i; \boldsymbol{\pi}_i)$  for  $i = 1, \dots, m$ , with  $\boldsymbol{\pi}_i \subseteq \boldsymbol{\pi}$ , the marginal densities of the approximation are

$$q_{\lambda_i}^0(\theta_i) = p_i(\vartheta_i; \boldsymbol{\pi}_i) t'_{\gamma_i}(\theta_i), \text{ for } i = 1, \dots, m, \quad (10)$$

with  $\boldsymbol{\lambda}_i^\top = (\boldsymbol{\gamma}_i^\top, \boldsymbol{\pi}_i^\top)$  a sub-vector of  $\boldsymbol{\lambda}^\top$ .

It is straightforward to show that the distribution with density at (9), has copula function

$$C(\mathbf{u}) = F(F_1^{-1}(u_1; \boldsymbol{\pi}_1), \dots, F_m^{-1}(u_m; \boldsymbol{\pi}_m); \boldsymbol{\pi}), \quad (11)$$

determined by  $F$ . Such a copula is called an ‘inversion copula’ by (Nelsen, 2006, pp.51–52) or an ‘implicit copula’ by (McNeil et al., 2005). We consider a Gaussian distribution for  $F$ , where  $F(\boldsymbol{\vartheta}; \boldsymbol{\pi}) = \Phi_m(\boldsymbol{\vartheta}; \boldsymbol{\mu}_\vartheta, \Sigma_\vartheta)$  is a Gaussian distribution function with mean  $\boldsymbol{\mu}_\vartheta$  and covariance matrix  $\Sigma_\vartheta$ . In this case (11) is the popular Gaussian copula function (Song, 2000), although alternative choices for  $F$  include other elliptical and skew-elliptical distributions resulting in different copula functions (Fang et al., 2002, Demarta and McNeil, 2005). Han et al. (2016) and Smith et al. (2020) point out that while density  $q_\lambda^0$  has a copula representation, it is more computationally efficient to utilize that at (9), and we do so here.

To allow for large  $m$ , we follow Miller et al. (2016) and Ong et al. (2018), and adopt a factor structure for  $\Sigma_\vartheta$  as follows. Let  $B$  be an  $m \times k$  matrix with  $k \ll m$ . For identifiability reasons it is assumed that the upper triangle of  $B$  is zero. Let  $\mathbf{d} = (d_1, \dots, d_m)^\top$  be a vector of parameters with  $d_i > 0$ , and denote by  $D$  the  $m \times m$  diagonal matrix with entries  $\mathbf{d}$ . We assume that

$$\Sigma_\vartheta = BB^\top + D^2, \quad (12)$$

so that the number of parameters in  $\Sigma_\vartheta$  grows only linearly with  $m$  if  $k \ll m$  is kept fixed. We note that this copula is equivalent to the Gaussian factor copula suggested by Murray et al. (2013) and Oh and Patton (2017) to model data, although they do not use it as a variational approximation. The Gaussian random vector has the generative representation  $\boldsymbol{\vartheta} = \boldsymbol{\mu}_\vartheta + B\boldsymbol{\zeta} + D\boldsymbol{\epsilon}$ , where  $\boldsymbol{\zeta} = (\zeta_1, \dots, \zeta_k)^\top \sim N(0, I_k)$  and  $\boldsymbol{\epsilon} \sim N(0, I_m)$ . By setting  $\boldsymbol{\varepsilon}^0 = (\boldsymbol{\zeta}^\top, \boldsymbol{\epsilon}^\top)^\top$ ,  $h^0(\boldsymbol{\varepsilon}^0, \boldsymbol{\lambda}) = (t_{\gamma_1}^{-1}(\vartheta_1), \dots, t_{\gamma_m}^{-1}(\vartheta_m))^\top$ , and  $\boldsymbol{\pi} = (\boldsymbol{\mu}_\vartheta^\top, \text{vech}(B)^\top, \mathbf{d}^\top)$ , closed form expressions for  $\frac{\partial \theta}{\partial \boldsymbol{\lambda}}$  and  $\nabla_\theta \log q_\lambda^0(\boldsymbol{\theta})$

required to compute (8) can be derived as in Appendix B. Here, the ‘vech’ operator is the half-vectorization of a rectangular matrix that simply vectorizes the non-zero elements of  $B$ .

Because  $\vartheta_i = t_{\gamma_i}(\theta_i)$  has a Gaussian distribution function  $F_i$ , we employ a transformation suggested by Yeo and Johnson (2000) (YJ hereafter) that has proven successful in transforming data to near normality. This extends the Box-Cox transformation to the entire real line and, for  $0 < \gamma < 2$ , is given by

$$t_{\gamma}(\theta) = \begin{cases} -\frac{(-\theta+1)^{2-\gamma}-1}{2-\gamma} & \text{if } \theta < 0 \\ \frac{(\theta+1)^{\gamma}-1}{\gamma} & \text{if } \theta \geq 0. \end{cases}$$

The transformation  $t_{\gamma} : \mathbb{R} \rightarrow \mathbb{R}$ , so that if a parameter  $\theta_i$  is constrained we first transform it to the real line; for example, with a scale or variance parameter we set  $\theta_i$  to its logarithm. When implementing SGA  $t_{\gamma}$  is not evaluated, but its inverse

$$t_{\gamma}^{-1}(\vartheta) = \begin{cases} 1 - (1 - \vartheta(2 - \gamma))^{1/(2-\gamma)} & \text{if } \vartheta < 0 \\ (1 + \vartheta\gamma)^{1/\gamma} - 1 & \text{if } \vartheta \geq 0, \end{cases}$$

is repeatedly. Monotonic nonparametric or flexible mixture transformations may also be used for  $t_{\gamma}$  (Han et al., 2016), but these can be much more difficult to calibrate jointly with  $\boldsymbol{\pi}$  for models with large numbers of latent variables than parametric choices, such as the YJ or inverse G&H (Tukey, 1977) transforms.

Algorithm 1 calibrates our proposed VA  $q_{\lambda}(\boldsymbol{\psi}) = q_{\lambda}^0(\boldsymbol{\theta})p(\mathbf{z}|\boldsymbol{\theta}, \mathbf{y})$  to the augmented posterior  $p(\boldsymbol{\psi}|\mathbf{y}) = p(\boldsymbol{\theta}, \mathbf{z}|\mathbf{y})$  using SGA with the re-parameterization trick and the ADADELTA learning rate.

## 2.4 Discussion of alternative variational approximations

The alternative of applying generic approximations to the augmented posterior  $p(\boldsymbol{\theta}, \mathbf{z}|\mathbf{y})$ , or the marginal posterior of the latent variables  $p(\mathbf{z}|\mathbf{y})$ , has been considered previously.

For example, Braun and McAuliffe (2010) do so for the posterior of a multinomial logistic regression augmented with random coefficient realizations, Hui et al. (2017) for latent variables in a generalized linear model, Loaiza-Maya and Smith (2019) for the augmented posterior of a discrete-margined copula model, and Archer et al. (2015) for the augmented posterior of a state space model, among others. Such approaches require a much larger number of variational parameters, result-

---

Initialize  $\boldsymbol{\lambda}^{(1)} = \left( \boldsymbol{\gamma}^{(1)}, \boldsymbol{\mu}_{\vartheta}^{(1)}, \text{vech}(B^{(1)}), \mathbf{d}^{(1)} \right)$ ,  $\mathbf{z}^{(0)}$  and set  $s = 1$ .

- (a) Generate  $\boldsymbol{\zeta}^{(s)} \sim N(0, I_k)$  and  $\boldsymbol{\epsilon}^{(s)} \sim N(0, I_m)$
  - (b) Compute  $\boldsymbol{\vartheta}^{(s)} = \boldsymbol{\mu}_{\vartheta}^{(s)} + B^{(s)}\boldsymbol{\zeta}^{(s)} + D^{(s)}\boldsymbol{\epsilon}^{(s)}$
  - (c) Compute  $\boldsymbol{\theta}^{(s)} = (t_{\gamma_1^{(s)}}^{-1}(\vartheta_1^{(s)}), \dots, t_{\gamma_m^{(s)}}^{-1}(\vartheta_m^{(s)}))^\top$  using the closed form inverse YJ transform
  - (d) Generate  $\mathbf{z}^{(s)} \sim p(\mathbf{z}|\boldsymbol{\theta}^{(s)}, \mathbf{y})$  (either exactly or approximately)
  - (e) Compute  $\nabla_{\boldsymbol{\lambda}} \widehat{\mathcal{L}}(\boldsymbol{\lambda}^{(s)}) = \frac{\partial \boldsymbol{\theta}}{\partial \boldsymbol{\lambda}}^\top \Big|_{\boldsymbol{\lambda}=\boldsymbol{\lambda}^{(s)}} \times [\nabla_{\boldsymbol{\theta}} \log g(\boldsymbol{\theta}^{(s)}, \mathbf{z}^{(s)}) - \nabla_{\boldsymbol{\theta}} \log q_{\boldsymbol{\lambda}^{(s)}}^0(\boldsymbol{\theta}^{(s)})]$
  - (f) Compute  $\Delta \boldsymbol{\lambda}^{(s)}$  using the ADADELTA method.
  - (g) Set  $\boldsymbol{\lambda}^{(s+1)} = \boldsymbol{\lambda}^{(s)} + \Delta \boldsymbol{\lambda}^{(s)}$ .
  - (h) Set  $s = s + 1$ . If stopping rule not satisfied go to step (a).
- 

**Algorithm 1:** SGA Algorithm to calibrate our proposed variational approximation

ing in three drawbacks compared to adopting the VA at (5). First, additional error is introduced into the variational estimate of  $p(\boldsymbol{\theta}|\mathbf{y})$  through imprecision in the approximation of the posterior of  $\mathbf{z}$ . Second, an increased computational burden at each step of the SGA algorithm because the re-parameterization gradient is a much larger vector than that at (8). Last, the SGA algorithm typically requires more steps, because additional noise is introduced into the Monte Carlo estimate of the gradient.

A seminal paper on variational inference for latent variable models is Hoffman et al. (2013). These authors consider mean field approximations in models with global model parameters and latent variables (which are called ‘local variables’), and describe how sub-sampling methods can be used in the variational optimization. Their method requires the model to have a conjugate exponential family structure. Hoffman and Blei (2015) consider structured stochastic variational inference methods where dependence between global parameters and local variables can be accommodated. They consider the possibility of using the exact conditional posterior for the latent variables as part of the approximation, similar to our approach, but unlike our method theirs also requires conjugacy, with MCMC sampling being used to estimate the expectations required in message passing algorithms.

Tan and Nott (2014) consider a stochastic variational inference implementation of non-conjugate variational message passing using sub-sampling which is useful for generalized linear mixed models, and some diagnostics for prior-data conflict checking.

Tan and Nott (2018) consider Gaussian VAs reflecting the true posterior conditional independence structure by parametrizing the precision matrix through a sparse Cholesky factor. Their methods apply to both random effects and state space models, and computations required for stochastic gradient lower bound optimization can be done efficiently. Tan et al. (2020) extend the method of Tan and Nott (2018) to non-Gaussian approximations through a sequential decomposition of the variational posterior. Each term in the decomposition is Gaussian, but variance parameters can be dependent on conditioning variables, which results in a non-Gaussian joint distribution. Tan (2017) considers some implementations of stochastic variational inference methods for discrete choice models, using an adaptive batch size where the batch size is increased as convergence is approached. Tan (2018) consider affine transformations for re-parametrizations of latent variable models which improve accuracy and where the functional form of the parametrization is deduced from a Taylor expansion. Roeder et al. (2019) consider variational inference for non-linear mixed effects and hierarchical models using factorized approximations and amortization to achieve scalability to large datasets.

Several authors have also considered variational approximations for the important class of generalized linear mixed models without using stochastic approximation methods for performing the variational optimization. Ormerod and Wand (2012) consider frequentist estimation in generalized linear mixed models, where random effects are integrated out in the marginal likelihood using a variational approach. The evidence lower bound can be computed using one-dimensional quadrature. Tan and Nott (2013) consider partially non-centred parametrizations within generalized linear mixed models to improve the accuracy of factorized Gaussian approximations and accelerate convergence, also using one-dimensional quadrature for lower bound computation. Kim and Wand (2018) consider expectation propagation methods for generalized linear mixed models and Nolan et al. (2019) consider efficient computations for mean field variational inference in models with multi-level random effects structures.

Tran et al. (2017) consider implementing variational inference when only an unbiased estimate of the likelihood is available. In the case of latent variable models such as random effects or state space models, unbiased estimates of the likelihood are obtained using importance sampling. A disadvantage of their approach is the need to adjust the Monte Carlo sample size in likelihood estimation to achieve constant variance of the corresponding log-likelihood estimate. This disadvantage is overcome in Gunawan et al. (2017). These authors consider sophisticated sub-sampling methods and variational inference algorithms implemented using re-parametrization gradients for large panel data models based on Fisher’s identity. Their method is most closely related to ours, and importance sampling methods are used for sampling conditional posterior distributions of the random effects. Their sub-sampling methods are related to similar methods in the MCMC literature (Quiroz et al., 2019). We do not consider sub-sampling here, but extend similar re-parametrization gradient estimation methods to those in Gunawan et al. (2017) beyond panel data models to more general latent variable models such as state space models, and consider MCMC methods rather than importance sampling for implementing conditional posterior simulation of latent variables.

There have been a number of general efforts to combine variational inference and MCMC. These include Salimans et al. (2015), Domke (2017), Li et al. (2017), Zhang and Hernández-Lobato (2018) and Ye et al. (2020) among others, although the methods do not focus specifically on computation for latent variable models. The method of Ruiz and Titsias (2019) does consider such models. The VA they consider corresponds to a parametrized approximation to an initial value of an MCMC algorithm which is run for a fixed small number of iterations. The variational parameters can be optimized to minimize a certain contrastive divergence between the approximation and true posterior. For the case of latent variable models, scalable amortized variational inference methods can be used in learning the variational parameters for the latent variables. Hoffman (2017) considers a method related to ours, where SGA algorithms are considered in which gradient estimates based on short MCMC runs starting from samples from a VA are considered. The approach is used for marginal maximum likelihood computations in deep latent Gaussian variable models.

### 3 Example: USCV Model for U.S. Inflation

Our first example illustrates the efficacy of our VB estimator for an unobserved component stochastic volatility (USCV) model for U.S. monthly inflation. This is an example of a nonlinear state space model, where mean-field approximations are known to be poor Wang and Titterton (2004), Karl et al. (2016). Previous authors have used structured Gaussian or other parametric VAs to the augmented posterior or marginal posterior of the latent states (Ghahramani and Hinton, 2000, Daunizeau et al., 2009, Archer et al., 2015, Naesseth et al., 2017). In contrast, our approach has a much lower number of variational parameters, involves less computation and provides greater accuracy than even well-structured parsimonious Gaussian approximations to the augmented posterior.

#### 3.1 The model

Let  $\mathbf{y} = (y_1, \dots, y_T)^\top$  be a time series of  $T = 874$  observations of monthly U.S. inflation from January 1947 to October 2019.<sup>4</sup> Many statistical models have been proposed for inflation, with variants of the USCV model among the most successful (Stock and Watson, 2007, Chan, 2013). We consider a stationary USCV with latent state  $\mathbf{z}_t = (\mu_t, \eta_t)^\top$  given by

$$\begin{aligned} y_t | \mathbf{z}_t, \boldsymbol{\theta} &\sim N(\mu_t, e^{\eta_t}) \\ \mu_t | \mu_{t-1}, \boldsymbol{\theta} &\sim N(\bar{\mu} + \rho_\mu(\mu_{t-1} - \bar{\mu}), \sigma_\mu^2) \\ \eta_t | \eta_{t-1}, \boldsymbol{\theta} &\sim N(\bar{\eta} + \rho_\eta(\eta_{t-1} - \bar{\eta}), \sigma_\eta^2), \end{aligned} \tag{13}$$

where we bound  $0 < \rho_\mu < 0.995$  and  $0 < \rho_\eta < 0.995$  for numerical stability. The parameters are  $\boldsymbol{\theta} = (\bar{\mu}, \kappa_\mu, \log(\sigma_\mu^2), \bar{\eta}, \kappa_\eta, \log(\sigma_\eta^2))^\top$ , where  $\kappa_\mu = \Phi^{-1}(\rho_\mu/0.995)$  and  $\kappa_\eta = \Phi^{-1}(\rho_\eta/0.995)$  are transformations of  $\rho_\mu$  and  $\rho_\eta$  to the real line to allow ready application of our VA. Proper uninformative priors are adopted as outlined in the Web Appendix.

#### 3.2 Estimation

Let  $\mathbf{z} = (\mathbf{z}_1^\top, \dots, \mathbf{z}_T^\top)^\top$ , then the augmented posterior

$$p(\boldsymbol{\theta}, \mathbf{z} | \mathbf{y}) \propto p(\boldsymbol{\theta}) \prod_{t=1}^T p(y_t | \mathbf{z}_t) p(\mathbf{z}_t | \mathbf{z}_{t-1}, \boldsymbol{\theta}), \tag{14}$$

---

<sup>4</sup>Inflation is measured as the continuously compounded change of the consumer price index for all urban consumers sourced from the FRED database.

is approximated by (5) with  $k = 2$  factors at (12), and  $\boldsymbol{\lambda}$  calibrated using Algorithm 1. At step (d) we draw  $\mathbf{z}$  by generating once from the closed form densities  $p(\boldsymbol{\mu}|\mathbf{y}, \boldsymbol{\theta}^{(s)}, \boldsymbol{\eta}^{(s-1)})$  and  $p(\boldsymbol{\eta}|\mathbf{y}, \boldsymbol{\theta}^{(s)}, \boldsymbol{\mu}^{(s)})$  that are given in the Web Appendix. While this provides only an approximate draw from  $p(\mathbf{z}|\boldsymbol{\theta}^{(s)}, \mathbf{y})$ , it is fast and we find it provides accurate estimates as documented below, although other approaches to generating a draw may also be used. When computing the re-parameterization gradient at (8),  $\nabla_{\boldsymbol{\theta}} \log g(\boldsymbol{\theta}, \mathbf{z})$  is available in closed form; see the Web Appendix.

While the likelihood of the UCSV model is intractable, exact posterior inference can be evaluated here using particle, MCMC or other methods (Chan, 2013, Kantas et al., 2015, Choppala et al., 2016, Katzfuss et al., 2019), and we do so to judge the accuracy of our VA. For comparison we also calibrate the structured Gaussian VA

$$q_{\lambda}(\boldsymbol{\theta}, \mathbf{z}) = \phi_m(\boldsymbol{\theta}; \boldsymbol{\mu}_{G,\theta}, \Sigma_G) \phi_{2T}(\mathbf{z}; \boldsymbol{\mu}_{G,z}, C_{G,z} C_{G,z}^{\top}) \quad (15)$$

where  $\phi_m(\cdot; \mathbf{a}, A)$  is the density of a  $m$ -dimensional  $N(\mathbf{a}, A)$  distribution,  $C_{G,z}$  is a band three lower triangular Cholesky factor, and a factor model with 3 factors is used for  $\Sigma_G$ . The approximation for  $\mathbf{z}$  introduces an additional  $(2T \times 4) - 3$  variational parameters that do not feature in (5).

### 3.3 Empirical results

#### 3.3.1 Estimates

Figure 1 plots the exact posterior mean of  $\mathbf{z}$ , along with the mean of  $\mathbf{z}$  for both calibrated VAs. Our proposed VA (labelled ‘Hybrid VA 1’) is much more accurate than the Gaussian VA. This is also the case when examining the marginal posteriors and their approximations, which are plotted in Figure 2. In particular, the approximation error for the log-volatilities  $\eta_1, \dots, \eta_T$  in the Gaussian VA evident in Figure 1(b) is matched by a substantial approximation error for their dynamic parameters  $\rho_{\eta}, \bar{\eta}, \sigma_{\eta}^2$  in Figure 2(a,b,c). Last, we explore the impact of drawing  $\mathbf{z}$  using multiple sweeps of a Gibbs sampler at step (d) of Algorithm 1. Figure 3 plots the means of the VAs of  $\mathbf{z}$  against their exact posterior means when 1, 10 and 100 sweeps of a Gibbs sampler are used at step (d). While a greater number of sweeps results in increased accuracy, it is only a minor improvement.



### 3.3.2 Accuracy and calibration speed

It is typical to judge the accuracy and calibration speed of different VAs using the lower bound  $\mathcal{L}$ . However, this is unavailable for the VA at (5) because the density  $p(\mathbf{z}|\boldsymbol{\theta}, \mathbf{y})$  is intractable. Therefore, we instead compute the accuracy of the one-step-ahead posterior predictive densities estimated using each VA. The predictive density is readily computed for the UCSV model as

$$\begin{aligned} p_{t+1|t}(y_{t+1}|\boldsymbol{\theta}, \mathbf{z}_t) &= \int \int p(y_{t+1}|\mu_{t+1}, \eta_{t+1}, \boldsymbol{\theta})p(\mu_{t+1}, \eta_{t+1}|\mu_t, \eta_t, \boldsymbol{\theta})d\mu_{t+1}d\eta_{t+1} \\ &= \int \phi_1(y_{t+1}; \bar{\mu} + \rho_\mu(\mu_t - \bar{\mu}), \sigma_\mu^2 + e^{\eta_{t+1}})\phi_1(\eta_{t+1}; \bar{\eta} + \rho_\eta(\eta_t - \bar{\eta}), \sigma_\eta^2)d\eta_{t+1}, \end{aligned}$$

where the integral in  $\eta_{t+1}$  is computed numerically. Then if the exact posterior means computed using MCMC are  $\bar{\boldsymbol{\theta}} = E(\boldsymbol{\theta}|\mathbf{y})$  and  $\bar{\mathbf{z}}_t = E(\mathbf{z}_t|\mathbf{y})$ , we measure the accuracy of a VA  $q_\lambda$  with mean  $\tilde{\boldsymbol{\theta}}, \tilde{\mathbf{z}}$  using the average Kullback-Leibler divergence  $\overline{\text{KL}}(\boldsymbol{\lambda}) = \frac{1}{T} \sum_{t=1}^T \text{KL}_{t+1|t}(\boldsymbol{\lambda})$ , where

$$\text{KL}_{t+1|t}(\boldsymbol{\lambda}) = \int p_{t+1|t}(y_t|\tilde{\boldsymbol{\theta}}, \tilde{\mathbf{z}}_t) \log \left( \frac{p_{t+1|t}(y_{t+1}|\tilde{\boldsymbol{\theta}}, \tilde{\mathbf{z}}_t)}{p_{t+1|t}(y_{t+1}|\bar{\boldsymbol{\theta}}, \bar{\mathbf{z}}_t)} \right) dy_{t+1},$$

is computed by numerical integration. Lower values of  $\overline{\text{KL}}(\boldsymbol{\lambda})$  suggest the VA  $q_\lambda$  has increased accuracy, with  $\overline{\text{KL}}(\boldsymbol{\lambda}) = 0$  when the VA  $q_\lambda(\boldsymbol{\theta}, \mathbf{z}) = p(\boldsymbol{\theta}, \mathbf{z}|\mathbf{y})$  is exact.

The minimum value of  $\overline{\text{KL}}(\boldsymbol{\lambda})$  was 0.0559 and 0.00029 for the Gaussian and our hybrid VA, respectively, so that our VA is substantially more accurate than the benchmark by this metric, consistent with the other empirical results given above. Last, Figure 4 plots  $\overline{\text{KL}}(\boldsymbol{\lambda})$  for all three VAs against (a) walk clock time, and also (b) step number for the SGA in Algorithm 1. It is evident that the Gaussian factor VA is not only less accurate, but slower to calibrate using SGA. Using an absolute change in  $\overline{\text{KL}}(\boldsymbol{\lambda})$  of 0.0001 as a stopping rule, coded in MATLAB and run on a standard laptop, the Gaussian VA took 4960 steps in 8.17s, whereas the Hybrid VA took 1403 steps in 1.73s. It is often observed in variational inference that more accurate VAs can be faster to calibrate using optimization methods.

## 4 Example: Mixed Tobit Model for Disaggregate Sales

Our second example applies our variational estimator to a mixed effects tobit (i.e. a censored regression) model for one million weekly sales amounts for a panel of 10,000 U.S. customers over  $T = 100$

weeks. The panel originates from Danaher et al. (2020) and these authors create a rich set of covariates that they model with both fixed and individual-level random coefficients. The authors point out that exact Bayesian estimation using MCMC is not computationally viable for the full dataset, and use variational inference with a structured Gaussian VA as in Ong et al. (2018). We show here that for a sub-sample of 100 individuals, our proposed VA is very close to the exact posterior and more accurate than either the Gaussian VA used by Danaher et al. (2020) or a mean field Gaussian VA. We then apply our approach to the full dataset and show it improves upon both Gaussian VAs.

## 4.1 The model

The response  $y_{it}$  for individual  $i = \{1, \dots, N\}$  at week  $t = \{1, \dots, T\}$  in a tobit model is an observation of a latent variable  $y_{it}^*$  censored at zero, so that  $y_{it} = y_{it}^*$  if  $y_{it}^* > 0$ , and  $y_{it} = 0$  if  $y_{it}^* \leq 0$ . The latent response follows a Gaussian mixed effects model

$$y_{it}^* = \mathbf{x}_{it}^\top \boldsymbol{\beta} + \mathbf{w}_{it}^\top \boldsymbol{\alpha}_i + \sigma \epsilon_{it}, \quad \epsilon_{it} \sim N(0, 1), \quad \boldsymbol{\alpha}_i \sim N(\mathbf{0}, V_\alpha),$$

where  $\mathbf{x}_{it}$  is a  $(p \times 1)$  vector of fixed effect covariates,  $\mathbf{w}_{it}$  is a  $(r \times 1)$  vector of random effect covariates that is a sub-vector of  $\mathbf{x}_{it}$ . Bayesian analysis of marketing panel data is popular because estimates of random coefficient values are often a key output (Manchanda et al., 2004, Danaher et al., 2015), as is the case here with  $\boldsymbol{\alpha} = (\boldsymbol{\alpha}_1^\top, \dots, \boldsymbol{\alpha}_N^\top)^\top$ . A Bayesian analysis requires specification of priors. Here we set  $V_\alpha = LL^\top + \Omega$ , with  $L$  a  $r \times k_\alpha$  factor loading matrix (with zeros in the upper triangle for identification) and the diagonal matrix  $\Omega = \text{diag}(\boldsymbol{\omega})$ , and then adopt independent uninformative priors for  $\text{vech}(L), \boldsymbol{\omega}, \boldsymbol{\beta}, \sigma^2$  as outlined in the Web Appendix.

## 4.2 Estimation

Let  $\mathbf{y}$  and  $\mathbf{y}^*$  be vectors of the  $n = NT$  values of  $y_{it}$  and  $y_{it}^*$ , respectively, and set  $\eta_{it} = \mathbf{x}_{it}^\top \boldsymbol{\beta} + \mathbf{w}_{it}^\top \boldsymbol{\alpha}_i$ . The likelihood  $p(\boldsymbol{\theta}|\mathbf{y})$  is intractable, so the focus is often on the posterior augmented with  $\boldsymbol{\alpha}$ , which has density

$$p(\boldsymbol{\alpha}, \boldsymbol{\theta}|\mathbf{y}) \propto \prod_{\{it:y_{it}=0\}} \Phi_1(0; \eta_{it}, \sigma^2) \prod_{\{it:y_{it}>0\}} \phi_1(y_{it}; \eta_{it}, \sigma^2) \prod_{i=1}^N \phi_r(\boldsymbol{\alpha}_i; \mathbf{0}, V_\alpha) p(\boldsymbol{\theta}). \quad (16)$$

In many marketing studies, including ours, weekly individual-level sales values  $y_{it}$  are mostly zero, so that the first product at (16) is over many more terms than the second product. For  $r$  and/or  $N$

large, integration over  $\boldsymbol{\alpha}$  to obtain the likelihood is computationally difficult, and MCMC methods that simulate  $\boldsymbol{\alpha}$  are popular.

It is often simpler and faster to consider the posterior augmented with both  $\boldsymbol{\alpha}$  and  $\mathbf{y}^*$ . This can be derived by first noting that  $p(\mathbf{y}^*|\mathbf{y}, \boldsymbol{\alpha}, \boldsymbol{\theta}) = \prod_{it} p(y_{it}^*|y_{it}, \boldsymbol{\alpha}, \boldsymbol{\theta})$ , with

$$p(y_{it}^*|y_{it}, \boldsymbol{\alpha}, \boldsymbol{\theta}) = \begin{cases} \frac{\phi_1(y_{it}^*; \eta_{it}, \sigma^2)}{\Phi_1(0; \eta_{it}, \sigma^2)} I(y_{it}^* \leq 0) & \text{for } y_{it}^* \leq 0 \\ I[y_{ij}^* = y_{it}] & \text{for } y_{it}^* > 0. \end{cases}$$

Then the augmented posterior is

$$p(\mathbf{y}^*, \boldsymbol{\alpha}, \boldsymbol{\theta}|\mathbf{y}) = p(\mathbf{y}^*|\mathbf{y}, \boldsymbol{\alpha}, \boldsymbol{\theta})p(\boldsymbol{\alpha}, \boldsymbol{\theta}|\mathbf{y}) \\ \propto \left[ \prod_{i=1, t=1}^{N, T} \phi_1(y_{it}^*; \eta_{it}, \sigma^2) \right] \left[ \prod_{i=1}^N \phi_r(\boldsymbol{\alpha}_i; \mathbf{0}, V_\alpha) \right] p(\sigma^2) p(\boldsymbol{\beta}) p(\text{vech}(L)) p(\boldsymbol{\omega}), \quad (17)$$

which was computed by substituting in the expressions above and cancelling terms. Using (17) a slow but simple Gibbs sampler for evaluating this augmented posterior exactly is given in the Web Appendix. However, even MCMC methods applied to either (16) or (17) become impractical for larger values of  $r$  and/or  $N$ , and in this case Danaher et al. (2020) propose using variational inference instead.

We estimate the model using our approach with  $\mathbf{z} = ((\mathbf{y}^*)^\top, \boldsymbol{\alpha}^\top)^\top$  and parameter vector  $\boldsymbol{\theta} = (\boldsymbol{\beta}^\top, \text{vech}(L)^\top, \boldsymbol{\omega}^\top, \sigma^2)^\top$ , where some elements are transformed to the real line for ready application of the VA as outlined in the Web Appendix. Thus, the VA is to the augmented posterior at (17). We use  $k = 10$  factors for the decomposition at (12). When implementing the SGA, at step (d) of Algorithm 1 we simulate  $\mathbf{z}$  from the conditionals  $p(\boldsymbol{\alpha} | (\mathbf{y}^*)^{(s-1)}, \boldsymbol{\theta}^{(s)}, \mathbf{y})$  and  $p(\mathbf{y}^* | \boldsymbol{\alpha}^{(s)}, \boldsymbol{\theta}^{(s)}, \mathbf{y})$  outlined in the Web Appendix. This is fast, and we undertake either 1, 5 or 10 sweeps of this simulation at step (d), forming a Gibbs sampler to produce a draw from  $p(\mathbf{z} | \boldsymbol{\theta}^{(s)}, \mathbf{y})$ .

We also include two additional Gaussian VAs to (16) as benchmarks. The first is that proposed by Danaher et al. (2020) with VA density  $q_{\boldsymbol{\lambda}}^G(\boldsymbol{\theta}, \boldsymbol{\alpha}) = q_{\boldsymbol{\lambda}^a}^{G,a}(\boldsymbol{\theta}) \prod_{i=1}^N q_{\boldsymbol{\lambda}^i}^{G,i}(\boldsymbol{\alpha})$ . Here,  $q_{\boldsymbol{\lambda}^a}^{G,a}$  and  $q_{\boldsymbol{\lambda}^i}^{G,i}$  are the densities of Gaussian factor VAs as in Ong et al. (2018), and  $\boldsymbol{\lambda}^\top = ((\boldsymbol{\lambda}^a)^\top, (\boldsymbol{\lambda}^1)^\top, \dots, (\boldsymbol{\lambda}^N)^\top)$ . Only one factor is used for  $q_{\boldsymbol{\lambda}^i}^{G,i}$ , while 10 factors are used for  $q_{\boldsymbol{\lambda}^a}^{G,a}$  to produce a richer approximation. The second benchmark is a simple Gaussian mean field VA, which is a popular choice in practice for models

with many parameters. Both benchmarks are calibrated using SGA with the re-parameterization trick as discussed in Ong et al. (2018).

### 4.3 Empirical results: small data

To assess the accuracy of our proposed VA we first consider a sample of only  $N = 100$  individuals observed over  $T = 100$  weeks. There are  $p = 32$  covariates which are described in the Web Appendix, and include measurements of an individual’s exposure to advertisements (ads) in three media (email, catalogs and paid search) to their in-store and online purchases for three retailer-brands (‘B1’, ‘B2’ and ‘B3’) in the clothing category. The response  $y_{it}$  is the logarithm of online spend plus one for retailer-brand B1 (called the focal brand here) by individual  $i$  in week  $t$ . We employ random coefficients at the individual consumer level for the three media ad exposure variables of the focal brand and the intercept, so that  $r = 4$ .

In this small data case, the exact posterior can be computed using a (slow) Gibbs sampler that generates from both  $\mathbf{y}^*$  and  $\boldsymbol{\alpha}$ ; see the Web Appendix. Figure 5 plots the exact posterior, and the three calibrated VAs, for three fixed effects coefficients and  $\sigma^2$ . The mean field VA is poor, greatly understating the posterior variance for all parameters, and located poorly for  $\sigma^2$ . The Gaussian VA is better, and our proposed VA (labelled ‘Hybrid’) is closest to the true posterior. Figure 6 presents the posteriors of the elements of  $V_{\alpha}$ , where there is a striking difference between the three VAs. Both Gaussian VAs under-estimate the level of posterior variance, and are incorrectly located for some elements, although the mean field VA is dramatically worse. In contrast, our proposed VA estimates the posteriors very well– not only getting the correct location and posterior variance, but also the posterior right skew correct for all elements of  $V_{\alpha}$ .

A key output of this model in Danaher et al. (2020) are the estimated random coefficient values  $\boldsymbol{\alpha}$ . To judge their accuracy, Figure 7 plots their  $rN = 400$  point estimates against their exact posterior means using our proposed VA when 1, 5 and 10 sweeps of the Gibbs sampler are used at step (d) of Algorithm 1. Increasing the number of sweeps improves the estimation accuracy of  $\boldsymbol{\alpha}$ , although a high degree is obtained with only 5 sweeps. Additional results for this example can be found in the Web Appendix.

## 4.4 Empirical results: full data

### 4.4.1 Estimates and inference

We now apply our method to the full dataset using the same response but for  $N = 10,000$  individuals and the same  $r = 10$  random coefficients considered by Danaher et al. (2020). Table 2 reports the estimates of  $\beta$  and  $\sigma$  for the three VAs. The results are broadly consistent, although the choice of VA affects some key parameters. For example, the coefficient of ‘Log Price’—a key effect in the original study—is  $-0.336$  with a 95% posterior interval of  $(-0.564, -0.073)$  using our VA, compared to  $-0.2$  with a 95% posterior interval of  $(-0.432, 0.031)$  using the Gaussian factor VA. Given the retail category is off-the-peg clothing, a significant negative coefficient is to be expected. Similarly, the coefficient of ‘B1 Catalog’ is twice as large in our analysis at  $1.452$ , compared to  $0.782$  using the Gaussian VA. This suggests that focal brand advertising through catalogs is twice as effective as the original results report.

Table 3 reports the estimate of  $V_\alpha$ . An objective of the original study was to measure the individual-level heterogeneity in the effects of focal and cross brand advertising, and we assess this here as a function of  $V_\alpha$  as follows. For individual  $i$ , let  $\mathbf{w}_{it}^{B1}$  be the three focal brand advertising spend covariates, and  $\mathbf{w}_{it}^{B23}$  be the six other brand advertising spend covariates. Further, let  $V_\alpha^{B1}$  and  $V_\alpha^{B23}$  be the corresponding sub-matrices of  $V_\alpha$ . Then for each VA we compute the distribution of the following three measures of heterogeneity:

$$\text{Total Heterogeneity: } \text{TH}(V_\alpha) = \frac{1}{Nr} \sum_{i,t} \mathbf{w}'_{it} V_\alpha \mathbf{w}_{it}.$$

$$\text{Focal Brand Ad Heterogeneity: } \text{FBH}(V_\alpha) = \frac{1}{Nr} \sum_{i,t} (\mathbf{w}_{it}^{B1})^\top V_\alpha^{B1} \mathbf{w}_{it}^{B1}.$$

$$\text{Cross Brand Ad Heterogeneity: } \text{CBH}(V_\alpha) = \frac{1}{Nr} \sum_{i,t} (\mathbf{w}_{it}^{B23})^\top V_\alpha^{B23} \mathbf{w}_{it}^{B23}.$$

Table 4 reports their estimates, and total heterogeneity is similar for both dependent VAs. However, the Hybrid VA estimates a substantially higher level of heterogeneity in advertising effectiveness, particularly for cross-brand advertising.

#### 4.4.2 Accuracy and calibration speed

We measure calibration accuracy and speed through the point predictions  $\hat{y}_{it} = E(y_{it}|\boldsymbol{\alpha}_i, \boldsymbol{\theta})$ , which can be calculated analytically from the tobit model, from which we can compute the root mean squared error  $\text{RMSE}(\boldsymbol{\alpha}, \boldsymbol{\theta}) = (\frac{1}{NT}(\sum_{i,t}(y_{i,t}-\hat{y}_{i,t})^2))^{1/2}$ . To judge the accuracy and speed of calibration we compute the RMSE for the values of  $\boldsymbol{\alpha}, \boldsymbol{\theta}$  obtained during the SGA. Figure 8 plots these values against both step number and clock time for all three VAs. By this metric, convergence of the SGA is several times faster for our proposed VA than the two Gaussian benchmarks.

## 5 Discussion

Variational inference has great potential for big models; especially those that employ a large number latent variables and use large datasets. However, popular mean field and structured Gaussian approximations for the augmented posterior can lack accuracy. To address this, we have described a new flexible and tractable variational family for large latent variable models. The marginal variational posterior distribution of the global parameters is specified using a Gaussian copula and non-Gaussian marginals, coupled with the exact conditional posterior distribution of the latent variables. The use of the latter removes much of the approximation error of the posterior distribution due to the latent variables, which can grow with the number of latents. We develop an efficient representation of the re-parameterization gradient, that allows the SGA algorithm to be implemented in a tractable way without requiring an expression for the conditional posterior density of  $\mathbf{z}$  or its gradient. The two applications demonstrate the good performance of our method.

There are interesting extensions to our method in several directions. First, variational methods for large data often use sub-sampling to avoid working with the whole dataset at each optimization step (Tan, 2017, Ansari et al., 2018). Sub-sampling is straightforward to implement with our method whenever the conditional posterior  $p(\mathbf{z}|\boldsymbol{\theta}, \mathbf{y})$  factorizes into a product density over the elements of  $\mathbf{z}$ , such as in many panel models. The use of sub-sampling would avoid the need to draw all the latent variables at step (d) of Algorithm 1, so that the method would be applicable to even larger datasets. A second extension of our methodology is to use new MCMC coupling methods (Jacob et al., 2020) at step (d) to compute exactly unbiased gradient estimates. Such coupling methods can be employed

when there is no convenient blocked Gibbs sampler available, and alternative methods like Hamiltonian Monte Carlo can be used for the MCMC implementation (Heng and Jacob, 2019). Combining coupling with sub-sampling may be particularly attractive, because the sampling then only needs to occur in a lower-dimensional space if all the latent variables do not need to be considered at once. Implementing such a scheme would involve a careful balance between reducing gradient variance, which requires sufficient large sub-samples, and reducing coupling times, which would require smaller sub-samples and hence sampling the conditional posterior for a lower-dimensional subset of the latent variables. Investigating the practicality of these ideas is left to future work.

## Appendix A Proof of Theorem 1

First, because  $\mathcal{L}(\boldsymbol{\lambda}) = \mathcal{L}^0(\boldsymbol{\lambda}) = E_{q_\lambda} [\log p(\mathbf{y}|\boldsymbol{\theta}) + \log p(\boldsymbol{\theta}) - \log q_\lambda^0(\boldsymbol{\theta})]$ , the re-parameterization gradient of  $\mathcal{L}$  is the same as that of  $\mathcal{L}^0$ , so that

$$\nabla_\lambda \mathcal{L}(\boldsymbol{\lambda}) = E_{f_{\boldsymbol{\varepsilon}^0}} \left\{ \frac{\partial \boldsymbol{\theta}^\top}{\partial \boldsymbol{\lambda}} [\nabla_\theta \log p(\boldsymbol{\theta}) + \nabla_\theta \log p(\mathbf{y}|\boldsymbol{\theta}) - \nabla_\theta \log q_\lambda^0(\boldsymbol{\theta})] \right\}. \quad (18)$$

Here, the random vector  $\boldsymbol{\varepsilon}^0$  has density  $f_{\boldsymbol{\varepsilon}^0}$  that does not depend on  $\boldsymbol{\lambda}$ , and  $h^0$  is the one-to-one vector-valued re-parameterization transformation from  $\boldsymbol{\varepsilon}^0$  to the parameter vector, such that  $\boldsymbol{\theta} = h^0(\boldsymbol{\varepsilon}^0, \boldsymbol{\lambda})$ .

Next, note that Fisher's identity gives (see, for example Equation (4) of Poyiadjis et al. (2011))

$$\nabla_\theta \log p(\mathbf{y}|\boldsymbol{\theta}) = \int \nabla_\theta [\log p(\mathbf{y}|\mathbf{z}, \boldsymbol{\theta}) p(\mathbf{z}|\boldsymbol{\theta})] p(\mathbf{z}|\boldsymbol{\theta}, \mathbf{y}) d\mathbf{z}$$

Substituting this expression into Equation (18), and writing  $E_{f_\boldsymbol{\varepsilon}}(\cdot)$  for expectation with respect to  $f_\boldsymbol{\varepsilon}(\boldsymbol{\varepsilon}) = f_{\boldsymbol{\varepsilon}^0}(\boldsymbol{\varepsilon}^0) p(\mathbf{z}|\boldsymbol{\theta}, \mathbf{y})$ , and because  $g(\boldsymbol{\theta}, \mathbf{z}) = p(\mathbf{y}|\mathbf{z}, \boldsymbol{\theta}) p(\mathbf{z}|\boldsymbol{\theta}) p(\boldsymbol{\theta})$ , we get

$$\begin{aligned} \nabla_\lambda \mathcal{L}(\boldsymbol{\lambda}) &= E_{f_\boldsymbol{\varepsilon}} \left\{ \frac{\partial \boldsymbol{\theta}^\top}{\partial \boldsymbol{\lambda}} [\nabla_\theta \log p(\boldsymbol{\theta}) + \nabla_\theta \log p(\mathbf{z}|\boldsymbol{\theta}) + \nabla_\theta \log p(\mathbf{y}|\mathbf{z}, \boldsymbol{\theta}) - \nabla_\theta \log q_\lambda^0(\boldsymbol{\theta})] \right\} \\ &= E_{f_\boldsymbol{\varepsilon}} \left\{ \frac{\partial \boldsymbol{\theta}^\top}{\partial \boldsymbol{\lambda}} [\nabla_\theta \log g(\boldsymbol{\theta}, \mathbf{z}) - \nabla_\theta \log q_\lambda^0(\boldsymbol{\theta})] \right\} \end{aligned}$$

which is the required result.

## Appendix B Terms Required in Theorem 1

Here we derive closed form expressions for two terms required to compute the re-parameterization gradient at (8) for our proposed VA. The third term,  $\nabla_\theta \log g(\boldsymbol{\theta}, \mathbf{z})$ , is computed from the augmented likelihood, and is therefore model specific.

### B.1 Computation of $\nabla_\theta \log q_\lambda^0(\boldsymbol{\theta})$

From (5), the assumption that  $\boldsymbol{\vartheta} \sim N(\boldsymbol{\mu}_\vartheta, \Sigma_\vartheta)$ , and the decomposition  $\Sigma_\vartheta = BB^\top + D^2$  at (12), then the gradient

$$\nabla_\theta \log q_\lambda^0(\boldsymbol{\theta}) = - \left[ \frac{\partial \boldsymbol{\vartheta}}{\partial \boldsymbol{\theta}} \right]^\top (BB^\top + D^2)^{-1} (\boldsymbol{\vartheta} - \boldsymbol{\mu}_\vartheta) + \left[ \frac{\partial}{\partial \boldsymbol{\theta}} \sum_{i=1}^m \log t'_{\gamma_i}(\theta_i) \right]^\top$$

where the diagonal matrix  $\frac{\partial \boldsymbol{\vartheta}}{\partial \boldsymbol{\theta}} = \text{diag}(t'_{\gamma_1}(\theta_1), \dots, t'_{\gamma_m}(\theta_m))$ . For the Yeo-Johnson transformation, the derivative

$$t'_\gamma(\theta) = \begin{cases} (-\theta + 1)^{1-\gamma} & \text{if } \theta < 0 \\ (\theta + 1)^{\gamma-1} & \text{if } \theta \geq 0, \end{cases}$$



so that  $\frac{\partial}{\partial \boldsymbol{\theta}} \sum_{i=1}^m \log t'_{\gamma_i}(\theta_i) = \left( \frac{\gamma_1-1}{|\theta_1|+1}, \dots, \frac{\gamma_m-1}{|\theta_m|+1} \right)$ . Following Ong et al. (2018), for large  $m$  the inverse of the  $m \times m$  matrix  $(BB^\top + D^2)$  (or the solutions of linear systems in this matrix) can be computed efficiently using the Woodbury formula

$$(BB^\top + D^2)^{-1} = D^{-2} - D^{-2}B(I + B^\top D^{-2}B)^{-1}B^\top D^{-2},$$

because  $(I + B^\top D^{-2}B)$  is a  $k \times k$  matrix with  $k \ll m$ .

## B.2 Computation of $\frac{\partial \boldsymbol{\theta}}{\partial \boldsymbol{\lambda}}^\top$

The variational parameter vector is  $\boldsymbol{\lambda} = (\boldsymbol{\mu}_\vartheta^\top, \text{vech}(B)^\top, \mathbf{d}^\top, \boldsymbol{\gamma}^\top)^\top$ , so that we compute the derivative of  $\boldsymbol{\theta}$  with respect to each of these four parameter vectors. To compute these first note that from the copula model and re-parameterization trick we can write

$$\boldsymbol{\theta} = t_\gamma^{-1}(\boldsymbol{\vartheta}) = t_\gamma^{-1}(\boldsymbol{\mu}_\vartheta + B\boldsymbol{\zeta} + D\boldsymbol{\epsilon}),$$

where we denote  $t_\gamma^{-1}(\boldsymbol{\vartheta}) \equiv (t_{\gamma_1}^{-1}(\vartheta_1), \dots, t_{\gamma_m}^{-1}(\vartheta_m))^\top$ . Then by repeated application of the chain rule

$$\begin{aligned} \text{(i)} \quad \frac{\partial \boldsymbol{\theta}}{\partial \boldsymbol{\mu}_\vartheta} &= \frac{\partial \boldsymbol{\theta}}{\partial \boldsymbol{\vartheta}} \frac{\partial \boldsymbol{\vartheta}}{\partial \boldsymbol{\mu}_\vartheta} = \frac{\partial \boldsymbol{\theta}}{\partial \boldsymbol{\vartheta}}, & \text{(ii)} \quad \frac{\partial \boldsymbol{\theta}}{\partial B} &= \frac{\partial \boldsymbol{\theta}}{\partial \boldsymbol{\vartheta}} \frac{\partial \boldsymbol{\vartheta}}{\partial B} = \frac{\partial \boldsymbol{\theta}}{\partial \boldsymbol{\vartheta}} (\boldsymbol{\zeta}^\top \otimes I_m) \\ \text{(iii)} \quad \frac{\partial \boldsymbol{\theta}}{\partial \mathbf{d}} &= \frac{\partial \boldsymbol{\theta}}{\partial \boldsymbol{\vartheta}} \frac{\partial \boldsymbol{\vartheta}}{\partial \mathbf{d}} = \frac{\partial \boldsymbol{\theta}}{\partial \boldsymbol{\vartheta}} \text{diag}(\boldsymbol{\epsilon}), & \text{(iv)} \quad \frac{\partial \boldsymbol{\theta}}{\partial \boldsymbol{\gamma}} &= -\frac{\partial \boldsymbol{\theta}}{\partial \boldsymbol{\vartheta}} \frac{\partial \boldsymbol{\vartheta}}{\partial \boldsymbol{\gamma}}, \end{aligned}$$

with the diagonal matrices  $\frac{\partial \boldsymbol{\theta}}{\partial \boldsymbol{\vartheta}} = \text{diag}(1/t'_{\gamma_1}(\theta_1), \dots, 1/t'_{\gamma_m}(\theta_m))$ ,  $\frac{\partial \boldsymbol{\vartheta}}{\partial \boldsymbol{\gamma}} = \text{diag}\left(\frac{\partial}{\partial \gamma_1} t_{\gamma_1}(\theta_1), \dots, \frac{\partial}{\partial \gamma_m} t_{\gamma_m}(\theta_m)\right)$  and  $\text{diag}(\boldsymbol{\epsilon})$ , where

$$\frac{\partial}{\partial \gamma} t_\gamma(\theta) = \begin{cases} \frac{(2-\gamma)(1-\theta)^{2-\gamma} \ln(1-\theta) - (1-\theta)^{2-\gamma} + 1}{(2-\gamma)^2} & \text{if } \theta < 0 \\ \frac{\gamma(1+\theta)^\gamma \ln(\theta+1) - (1+\theta)^\gamma + 1}{\gamma^2} & \text{if } \theta \geq 0. \end{cases}$$

Notice that evaluation of the derivatives at (i)–(iv) above only involves sparse matrix computations, which can be employed for larger values of  $m$  in practice. Last, to obtain  $\frac{\partial \boldsymbol{\theta}}{\partial \text{vech}(B)}$  simply extract the corresponding elements from  $\frac{\partial \boldsymbol{\theta}}{\partial B}$ .

## References

- Allenby, G. M. and Rossi, P. E. (1998). Marketing models of consumer heterogeneity. *Journal of econometrics*, 89(1-2):57–78.
- Ansari, A., Li, Y., and Zhang, J. Z. (2018). Probabilistic topic model for hybrid recommender systems: A stochastic variational Bayesian approach. *Marketing Science*, 37(6):987–1008.
- Archer, E., Park, I. M., Buesing, L., Cunningham, J., and Paninski, L. (2015). Black box variational inference for state space models. *arXiv preprint arXiv:1511.07367*.
- Blei, D. M., Kucukelbir, A., and McAuliffe, J. D. (2017). Variational inference: A review for statisticians. *Journal of the American Statistical Association*, 112(518):859–877.
- Bottou, L. (2010). Large-scale machine learning with stochastic gradient descent. In Lechevallier, Y. and Saporta, G., editors, *Proceedings of the 19th International Conference on Computational Statistics (COMPSTAT'2010)*, pages 177–187. Springer.
- Braun, M. and McAuliffe, J. (2010). Variational inference for large-scale models of discrete choice. *Journal of the American Statistical Association*, 105:324–335.
- Chan, J. C. (2013). Moving average stochastic volatility models with application to inflation forecast. *Journal of Econometrics*, 176(2):162–172.
- Choppala, P., Gunawan, D., Chen, J., Tran, M.-N., and Kohn, R. (2016). Bayesian inference for state space models using block and correlated pseudo marginal methods. *arXiv preprint arXiv:1612.07072*.
- Danaher, P. J., Danaher, T. S., Smith, M. S., and Loaiza-Maya, R. (2020). Advertising effectiveness for multiple retailer-brands in a multimedia and multichannel environment. *Journal of Marketing Research*, in press.
- Danaher, P. J., Smith, M. S., Ranasinghe, K., and Danaher, T. S. (2015). Where, when, and how long: Factors that influence the redemption of mobile phone coupons. *Journal of Marketing Research*, 52(5):710–725.
- Daunizeau, J., Friston, K. J., and Kiebel, S. J. (2009). Variational Bayesian identification and prediction of stochastic nonlinear dynamic causal models. *Physica D: nonlinear phenomena*, 238(21):2089–2118.
- Demarta, S. and McNeil, A. J. (2005). The t copula and related copulas. *International Statistical Review*, 73(1):111–129.
- Domke, J. (2017). A divergence bound for hybrids of MCMC and variational inference and an application to Langevin dynamics and SGVI. In *Proceedings of the 34th International Conference on Machine Learning - Volume 70, ICML'17*, page 1029–1038. JMLR.org.
- Durbin, J. and Koopman, S. J. (2012). *Time series analysis by state space methods*. Oxford University Press.

- Fang, H.-B., Fang, K.-T., and Kotz, S. (2002). The meta-elliptical distributions with given marginals. *Journal of Multivariate Analysis*, 82(1):1–16.
- Gelman, A. and Hill, J. (2006). *Data analysis using regression and multilevel/hierarchical models*. Cambridge University Press.
- Ghahramani, Z. and Hinton, G. E. (2000). Variational learning for switching state-space models. *Neural computation*, 12(4):831–864.
- Gunawan, D., Tran, M.-N., and Kohn, R. (2017). Fast inference for intractable likelihood problems using variational Bayes. *arXiv preprint arXiv:1705.06679*.
- Han, S., Liao, X., Dunson, D., and Carin, L. (2016). Variational Gaussian copula inference. In Gretton, A. and Robert, C. C., editors, *Proceedings of the 19th International Conference on Artificial Intelligence and Statistics*, volume 51 of *Proceedings of Machine Learning Research*, pages 829–838, Cadiz, Spain. PMLR.
- Heng, J. and Jacob, P. E. (2019). Unbiased Hamiltonian Monte Carlo with couplings. *Biometrika*, 106(2):287–302.
- Hoffman, M. and Blei, D. (2015). Stochastic structured variational inference. In Lebanon, G. and Vishwanathan, S. V. N., editors, *Proceedings of the Eighteenth International Conference on Artificial Intelligence and Statistics*, volume 38 of *Proceedings of Machine Learning Research*, pages 361–369, San Diego, California, USA. PMLR.
- Hoffman, M. D. (2017). Learning deep latent Gaussian models with Markov chain Monte Carlo. In Precup, D. and Teh, Y. W., editors, *Proceedings of the 34th International Conference on Machine Learning*, volume 70 of *Proceedings of Machine Learning Research*, pages 1510–1519. PMLR.
- Hoffman, M. D., Blei, D. M., Wang, C., and Paisley, J. (2013). Stochastic variational inference. *The Journal of Machine Learning Research*, 14(1):1303–1347.
- Hui, F. K., Warton, D. I., Ormerod, J. T., Haapaniemi, V., and Taskinen, S. (2017). Variational approximations for generalized linear latent variable models. *Journal of Computational and Graphical Statistics*, 26(1):35–43.
- Jacob, P. E., O’Leary, J., and Atchadé, Y. F. (2020). Unbiased Markov chain Monte Carlo with couplings (with discussion). *Journal of the Royal Statistical Society, Series B*, (forthcoming).
- Kantas, N., Doucet, A., Singh, S. S., Maciejowski, J., Chopin, N., et al. (2015). On particle methods for parameter estimation in state-space models. *Statistical science*, 30(3):328–351.
- Karl, M., Soelch, M., Bayer, J., and Van der Smagt, P. (2016). Deep variational Bayes filters: Unsupervised learning of state space models from raw data. *arXiv preprint arXiv:1605.06432*.
- Katzfuss, M., Stroud, J. R., and Wikle, C. K. (2019). Ensemble Kalman methods for high-dimensional hierarchical dynamic space-time models. *Journal of the American Statistical Association*, pages 1–43.

- Kim, A. S. and Wand, M. P. (2018). On expectation propagation for generalised, linear and mixed models. *Australian and New Zealand Journal of Statistics*, 60:75–102.
- Kingma, D. P. and Welling, M. (2014). Auto-encoding variational Bayes. *arXiv preprint arXiv:1312.6114*.
- Kucukelbir, A., Tran, D., Ranganath, R., Gelman, A., and Blei, D. M. (2017). Automatic differentiation variational inference. *Journal of Machine Learning Research*, 18(14):1–45.
- Li, Y., Turner, R. E., and Liu, Q. (2017). Approximate inference with amortised MCMC. *arXiv preprint arXiv:1702.08343*.
- Loaiza-Maya, R. and Smith, M. S. (2019). Variational Bayes estimation of discrete-margined copula models with application to time series. *Journal of Computational and Graphical Statistics*, 28(3):523–539.
- Manchanda, P., Rossi, P. E., and Chintagunta, P. K. (2004). Response modeling with nonrandom marketing-mix variables. *Journal of Marketing Research*, 41(4):467–478.
- McNeil, A. J., Frey, R., and Embrechts, P. (2005). *Quantitative Risk Management: Concepts, Techniques and Tools*. Princeton Series in Finance.
- Miller, A. C., Foti, N., and Adams, R. P. (2016). Variational boosting: Iteratively refining posterior approximations. arXiv: 1611.06585.
- Molenberghs, G. and Verbeke, G. (2006). *Models for discrete longitudinal data*. Springer Science & Business Media.
- Murray, J. S., Dunson, D. B., Carin, L., and Lucas, J. E. (2013). Bayesian Gaussian copula factor models for mixed data. *Journal of the American Statistical Association*, 108(502):656–665.
- Naesseth, C. A., Linderman, S. W., Ranganath, R., and Blei, D. M. (2017). Variational Sequential Monte Carlo. *arXiv preprint arXiv:1705.11140*.
- Nelsen, R. B. (2006). *An Introduction to Copulas (Springer Series in Statistics)*. Springer-Verlag New York, Inc., Secaucus, NJ, USA.
- Nolan, T. H., Menictas, M., and Wand, M. P. (2019). Streamlined computing for variational inference with higher level random effects. *arXiv preprint arXiv:1903.06616*.
- Nott, D. J., Tan, S. L., Villani, M., and Kohn, R. (2012). Regression Density Estimation with Variational Methods and Stochastic Approximation. *Journal of Computational and Graphical Statistics*, 21(3):797–820.
- Oh, D. H. and Patton, A. J. (2017). Modeling Dependence in High Dimensions With Factor Copulas. *Journal of Business & Economic Statistics*, 35(1):139–154.
- Ong, V. M.-H., Nott, D. J., and Smith, M. S. (2018). Gaussian variational approximation with a factor covariance structure. *Journal of Computational and Graphical Statistics*, 27(3):465–478.

- Ormerod, J. T. and Wand, M. P. (2010). Explaining variational approximations. *The American Statistician*, 64(2):140–153.
- Ormerod, J. T. and Wand, M. P. (2012). Gaussian variational approximate inference for generalized linear mixed models. *Journal of Computational and Graphical Statistics*, 21(1):2–17.
- Paisley, J., Blei, D. M., and Jordan, M. I. (2012). Variational Bayesian inference with stochastic search. In *Proceedings of the 29th International Conference on Machine Learning (ICML-12)*, pages 1363–1370.
- Poyiadjis, G., Doucet, A., and Singh, S. S. (2011). Particle approximations of the score and observed information matrix in state space models with application to parameter estimation. *Biometrika*, 98(1):65–80.
- Quiroz, M., Kohn, R., Villani, M., and Tran, M.-N. (2019). Speeding up MCMC by efficient data subsampling. *Journal of the American Statistical Association*, 114(526):831–843.
- Quiroz, M., Nott, D. J., and Kohn, R. (2018). Gaussian variational approximation for high-dimensional state space models. arXiv: 1801.07873.
- Ranganath, R., Gerrish, S., and Blei, D. (2014). Black Box Variational Inference. In *Artificial Intelligence and Statistics*, pages 814–822.
- Rezende, D. J., Mohamed, S., and Wierstra, D. (2014). Stochastic backpropagation and approximate inference in deep generative models. In Xing, E. P. and Jebara, T., editors, *Proceedings of the 31st International Conference on Machine Learning*, volume 32 of *Proceedings of Machine Learning Research*, pages 1278–1286, Beijing, China. PMLR.
- Robbins, H. and Monro, S. (1951). A stochastic approximation method. *The Annals of Mathematical Statistics*, 22(3):400–407.
- Roeder, G., Grant, P. K., Phillips, A., Dalchau, N., and Meeds, E. (2019). Efficient amortised Bayesian inference for hierarchical and nonlinear dynamical systems. In Chaudhuri, K. and Salakhutdinov, R., editors, *Proceedings of the 36th International Conference on Machine Learning, ICML 2019, 9-15 June 2019, Long Beach, California, USA*, volume 97 of *Proceedings of Machine Learning Research*, pages 4445–4455. PMLR.
- Rossi, P. E., McCulloch, R. E., and Allenby, G. M. (1996). The value of purchase history data in target marketing. *Marketing Science*, 15(4):321–340.
- Ruiz, F. and Titsias, M. (2019). A contrastive divergence for combining variational inference and MCMC. In Chaudhuri, K. and Salakhutdinov, R., editors, *Proceedings of the 36th International Conference on Machine Learning*, volume 97 of *Proceedings of Machine Learning Research*, pages 5537–5545, Long Beach, California, USA. PMLR.
- Salimans, T., Kingma, D., and Welling, M. (2015). Markov chain Monte Carlo and variational inference: Bridging the gap. In *Proceedings of the 32nd International Conference on Machine Learning (ICML-15)*, pages 1218–1226.

- Salimans, T., Knowles, D. A., et al. (2013). Fixed-form variational posterior approximation through stochastic linear regression. *Bayesian Analysis*, 8(4):837–882.
- Smith, M. S., Loaiza-Maya, R., and Nott, D. J. (2020). High-dimensional copula variational approximation through transformation. *Journal of Computational and Graphical Statistics*, forthcoming.
- Song, X.-K. P. (2000). Multivariate dispersion models generated from Gaussian copula. *Scandinavian Journal of Statistics*, 27(2):305–320.
- Stock, J. H. and Watson, M. W. (2007). Why Has U.S. Inflation Become Harder to Forecast? *Journal of Money, Credit and Banking*, 39(s1):3–33.
- Tan, L. S. L. (2017). Stochastic variational inference for large-scale discrete choice models using adaptive batch sizes. *Statistics and Computing*, 27:237–257.
- Tan, L. S. L. (2018). Use of model reparametrization to improve variational Bayes. *arXiv preprint arXiv:1805.07267*.
- Tan, L. S. L., Bhaskaran, A., and Nott, D. J. (2020). Conditionally structured variational Gaussian approximation with importance weights. *Statistics and Computing*, (forthcoming).
- Tan, L. S. L. and Nott, D. J. (2013). Variational inference for generalized linear mixed models using partially noncentered parametrizations. *Statistical Science*, 28(2):168–188.
- Tan, L. S. L. and Nott, D. J. (2014). A stochastic variational framework for fitting and diagnosing generalized linear mixed models. *Bayesian Analysis*, 9(4):963–1004.
- Tan, L. S. L. and Nott, D. J. (2018). Gaussian variational approximation with sparse precision matrices. *Statistics and Computing*, 28(2):259–275.
- Titsias, M. and Lázaro-Gredilla, M. (2014). Doubly stochastic variational Bayes for non-conjugate inference. In Xing, E. P. and Jebara, T., editors, *Proceedings of the 31st International Conference on Machine Learning*, volume 32 of *Proceedings of Machine Learning Research*, pages 1971–1979, Beijing, China. PMLR.
- Train, K. E. (2009). *Discrete choice methods with simulation*. Cambridge University Press.
- Tran, M.-N., Nott, D. J., and Kohn, R. (2017). Variational Bayes with intractable likelihood. *Journal of Computational and Graphical Statistics*, 26(4):873–882.
- Tukey, T. W. (1977). Modern techniques in data analysis. NSP-sponsored regional research conference at Southeastern Massachusetts University, North Dartmouth, Massachusetts.
- Wang, B. and Titterton, D. (2004). Lack of consistency of mean field and variational Bayes approximations for state space models. *Neural Processing Letters*, 20(3):151–170.
- Wang, Y. and Blei, D. (2019). Variational Bayes under model misspecification. In Wallach, H., Larochelle, H., Beygelzimer, A., d’Alché Buc, F., Fox, E., and Garnett, R., editors, *Advances in Neural Information Processing Systems 32*, pages 13357–13367. Curran Associates, Inc.

- Xu, M., Quiroz, M., Kohn, R., and Sisson, S. A. (2018). On some variance reduction properties of the reparameterization trick. *arXiv preprint arXiv:1809.10330*.
- Ye, L., Beskos, A., De Iorio, M., and Hao, J. (2020). *Statistics and Computing*, (forthcoming).
- Yeo, I.-K. and Johnson, R. A. (2000). A new family of power transformations to improve normality or symmetry. *Biometrika*, 87(4):954–959.
- Zeiler, M. D. (2012). ADADELTA: An adaptive learning rate method. arXiv:1212.5701.
- Zhang, Y. and Hernández-Lobato, J. M. (2018). Ergodic inference: Accelerate convergence by optimisation. *arXiv preprint arXiv:1805.10377*.

Table 1: Accuracy and speed of variational inference for the UCSV model of U.S. inflation

Var. Approx.	$\min_{\lambda}(\overline{\text{KL}}(\boldsymbol{\lambda}))$	Steps to Stop	Time to Stop
Structured Gaussian	0.0559	4960	8.17 sec
Hybrid	0.0003	1403	1.73 sec

The two VAs are a structured Gaussian approximation to the augmented posterior and our proposal labelled ‘Hybrid’. The first column reports the minimum average KL divergence (as defined in the text) between each calibrated VA and the exact posterior evaluated using MCMC. The second and third columns report the number of steps and clock time, for the SGA to stop using an absolute change of  $\overline{\text{KL}}(\boldsymbol{\lambda})$  less than 0.0001 as a stopping rule.



	Hybrid VA			Gaussian VA			Gaussian MF VA		
	Mean	5%	95%	Mean	5%	95%	Mean	5%	95%
Intercept	-15.71	-16.42	-14.99	-16.36	-17.12	-15.59	-16.31	-16.35	-16.27
<i>Lagged Sales</i>									
B1 past D sales	0.177	0.147	0.206	0.179	0.179	0.179	0.184	0.160	0.208
B2 past D sales	0.109	0.055	0.162	0.117	0.073	0.160	0.126	0.080	0.172
B3 past D sales	0.113	0.071	0.155	0.111	0.073	0.149	0.113	0.075	0.151
B1 past R sales	0.137	0.130	0.143	0.150	0.143	0.158	0.174	0.168	0.181
B2 past R sales	0.072	0.021	0.121	0.073	0.031	0.114	0.084	0.040	0.128
B3 past R sales	0.101	0.068	0.133	0.098	0.087	0.109	0.102	0.077	0.128
<i>Ad Variables</i>									
B1 Emails	1.756	1.641	1.867	1.797	1.775	1.820	1.142	1.107	1.176
B1 Catal.	1.452	1.084	1.790	0.782	0.588	0.972	0.931	0.741	1.117
B1 Paid S.	0.921	0.291	1.437	0.716	0.354	1.084	0.485	0.173	0.801
B2 Emails	-0.521	-0.687	-0.339	-0.431	-0.497	-0.366	-0.135	-0.200	-0.072
B2 Catal.	-1.069	-1.505	-0.562	-0.899	-1.152	-0.646	-0.354	-0.598	-0.109
B2 Paid S.	-1.354	-3.113	0.306	0.183	-0.764	1.114	0.501	-0.413	1.389
B3 Emails	-0.565	-0.676	-0.448	-0.602	-0.639	-0.565	-0.335	-0.372	-0.297
B3 Catal.	-1.201	-1.581	-0.776	-1.012	-1.257	-0.765	-0.524	-0.760	-0.285
B3 Paid S.	-0.054	-1.181	0.991	0.017	-0.736	0.768	0.184	-0.543	0.917
<i>Endog. Controls</i>									
Res Paid S.	0.008	-0.085	0.097	0.006	-0.064	0.076	0.044	-0.023	0.112
Organic S. CFs	1.628	1.356	1.882	1.600	1.421	1.781	1.621	1.440	1.803
Res Organic S.	0.334	0.227	0.436	0.345	0.251	0.437	0.347	0.251	0.442
Res website V.	0.188	0.116	0.258	0.198	0.135	0.261	0.218	0.156	0.280
Visits B1	1.832	1.736	1.928	1.839	1.777	1.902	1.846	1.782	1.910
<i>Other Variables</i>									
log price	-0.336	-0.564	-0.073	-0.200	-0.432	0.031	-0.216	-0.224	-0.208
month1	-0.932	-1.110	-0.743	-0.925	-1.086	-0.765	-0.895	-1.040	-0.752
month2	-0.834	-0.988	-0.668	-0.834	-0.988	-0.685	-0.849	-0.986	-0.710
month3	-0.417	-0.577	-0.245	-0.430	-0.612	-0.252	-0.446	-0.575	-0.317
month4	-0.299	-0.455	-0.125	-0.302	-0.464	-0.140	-0.324	-0.457	-0.192
month5	0.092	-0.078	0.244	0.102	-0.043	0.247	0.069	-0.054	0.191
month7	0.081	-0.151	0.284	0.052	-0.172	0.277	0.043	-0.141	0.226
month8	0.083	-0.084	0.235	0.082	-0.062	0.225	0.055	-0.065	0.174
month9	-0.200	-0.362	-0.019	-0.219	-0.394	-0.045	-0.244	-0.376	-0.114
month10	-0.203	-0.377	-0.008	-0.228	-0.409	-0.049	-0.238	-0.373	-0.104
month11	0.166	-0.010	0.321	0.140	-0.029	0.312	0.144	0.025	0.261
month12	1.744	1.595	1.891	1.793	1.645	1.943	1.777	1.669	1.883
$\sigma$	7.698	7.665	7.731	7.755	7.725	7.784	7.801	7.789	7.812

Table 2: Variational mean and quantiles for  $\beta$  in the full data Tobit example. The variables ( $\mathbf{x}_{it}$ ) are defined in the Web Appendix. Results are given for our approach (Hybrid VA), the Gaussian factor VA of Danaher et al. (2020) and mean field VA. The estimated error standard deviation  $\sigma$  is also reported.

Table 3: Estimate of  $V_\alpha$  for the full data Tobit example using our proposed VA.

	Intercept	Emails	B1 Catal.	Paid S.	Emails	B2 Catal.	Paid S.	Emails	B3 Catal.	Paid S.
Intercept	28.412 (27.38, 29.68)	-	-	-	-	-	-	-	-	-
Emails	-0.624 (-0.66, -0.58)	2.814 (2.47, 3.18)	-	-	-	-	-	-	-	-
B1 Catal.	-0.519 (-0.75, -0.28)	0.435 (0.19, 0.63)	4.041 (1.43, 9.64)	-	-	-	-	-	-	-
Paid S.	-0.289 (-0.58, -0.01)	0.231 (-0.02, 0.48)	0.187 (-0.41, 0.65)	3.509 (0.93, 9.15)	-	-	-	-	-	-
Emails	0.341 (0.15, 0.53)	-0.291 (-0.47, -0.12)	-0.234 (-0.57, 0.16)	-0.094 (-0.45, 0.3)	1.335 (0.73, 2.13)	-	-	-	-	-
B2 Catal.	0.388 (0.12, 0.68)	-0.27 (-0.53, -0.02)	-0.164 (-0.71, 0.39)	-0.107 (-0.69, 0.54)	0.152 (-0.28, 0.53)	5.175 (1.52, 13.51)	-	-	-	-
Paid S.	0.45 (0.02, 0.77)	-0.375 (-0.64, 0.05)	-0.368 (-0.83, 0.36)	-0.148 (-0.74, 0.57)	0.246 (-0.23, 0.63)	0.212 (-0.52, 0.82)	13.377 (2.25, 39.15)	-	-	-
Emails	0.322 (0.18, 0.47)	-0.272 (-0.4, -0.14)	-0.247 (-0.54, 0.11)	-0.173 (-0.52, 0.21)	0.14 (-0.11, 0.36)	0.079 (-0.34, 0.45)	0.192 (-0.3, 0.57)	0.67 (0.43, 1.09)	-	-
B3 Catal.	0.425 (0.15, 0.71)	-0.326 (-0.59, -0.02)	-0.336 (-0.79, 0.3)	-0.133 (-0.68, 0.5)	0.174 (-0.27, 0.55)	0.189 (-0.49, 0.75)	0.232 (-0.51, 0.8)	0.122 (-0.3, 0.48)	4.261 (1.21, 10.61)	-
Paid S.	-0.088 (-0.5, 0.34)	0.107 (-0.25, 0.43)	0.118 (-0.57, 0.74)	-0.058 (-0.71, 0.64)	-0.056 (-0.48, 0.4)	-0.022 (-0.75, 0.69)	-0.087 (-0.79, 0.73)	-0.043 (-0.49, 0.44)	0.063 (-0.66, 0.77)	7.784 (1.16, 23.42)

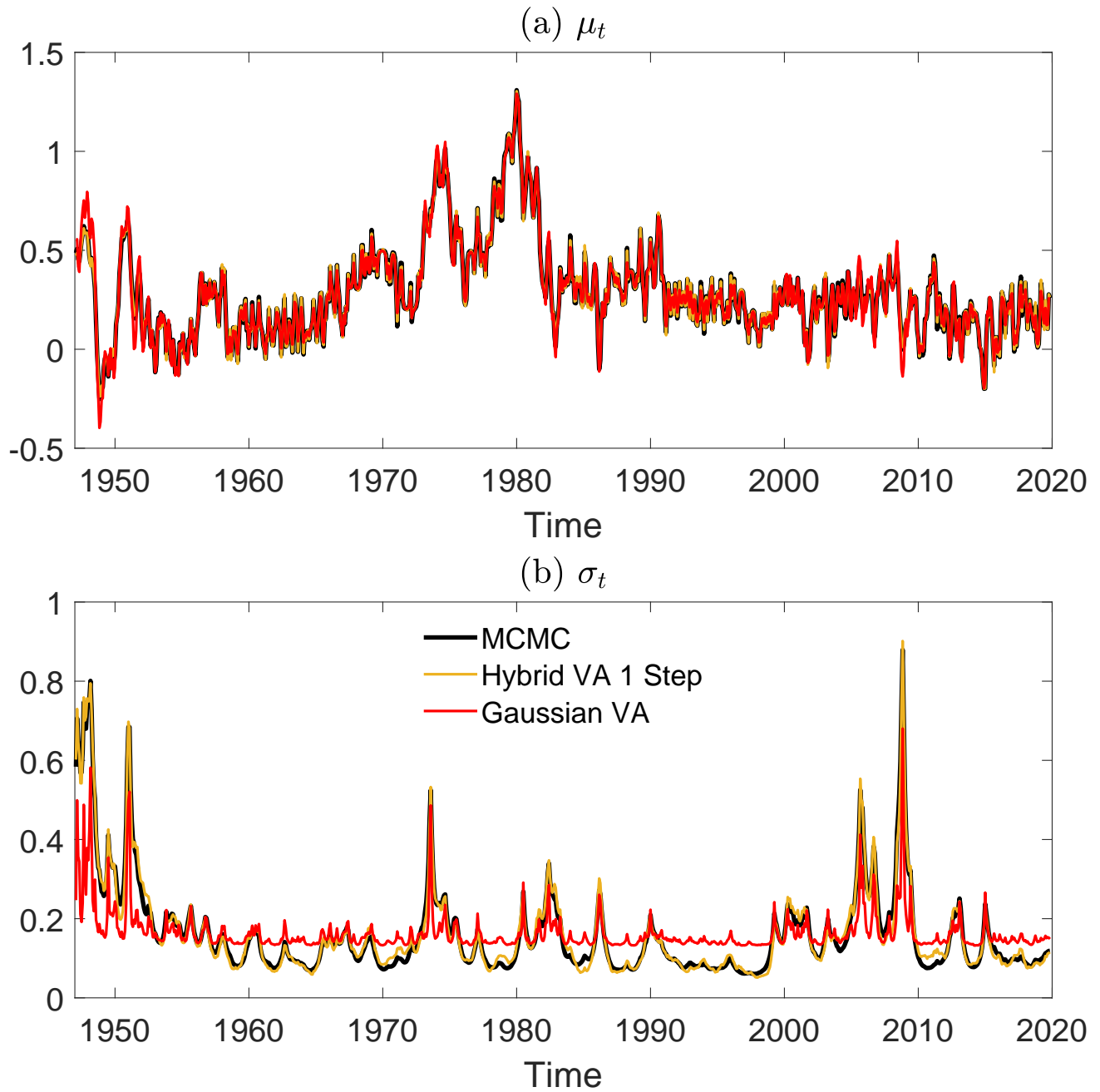
The diagonal values are estimates of the variances of the random coefficients (i.e. the leading diagonal of  $V_\alpha$ ). The off-diagonal values are estimates of the correlations between the random coefficients (i.e. the correlations of the matrix  $V_\alpha$ ). The variational means are reported, along with the 95% quantiles of the variational distribution  $q_\lambda$  in parentheses.

Table 4: Heterogeneity estimates for the full data Tobit example.

	TH	FBH	CBH
Hybrid VA	29.506 <i>(28.50, 30.93)</i>	2.647 <i>(2.32, 3.02)</i>	1.677 <i>(1.27, 2.32)</i>
Gaussian VA	28.252 <i>(27.92, 28.59)</i>	2.320 <i>(2.27, 2.38)</i>	0.663 <i>(0.65, 0.67)</i>
Gaussian MF VA	25.212 <i>(24.26, 26.31)</i>	0.040 <i>(0.04, 0.04)</i>	0.108 <i>(0.106, 0.11)</i>

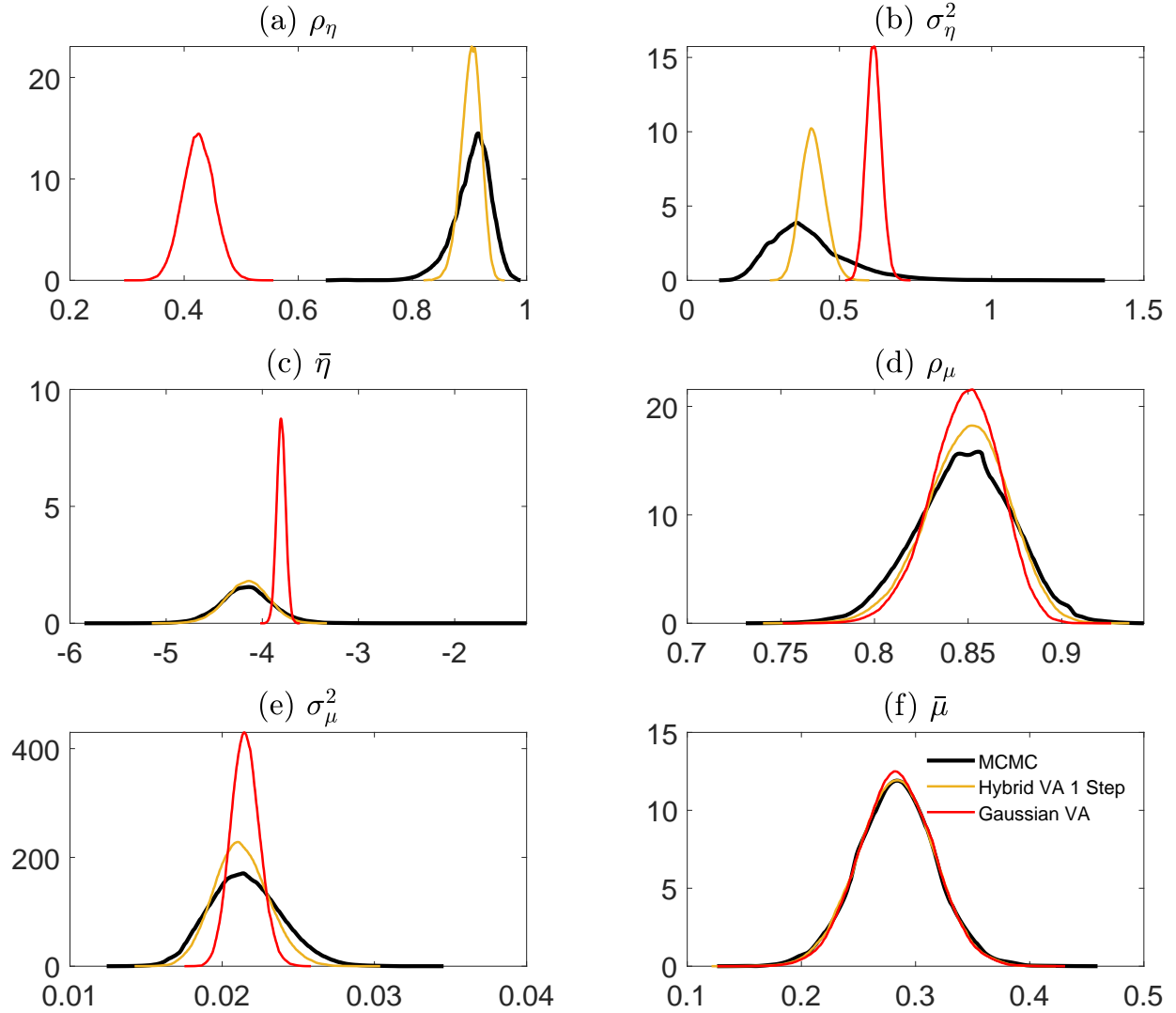
The variational mean of the three heterogeneity measures  $\text{TH}(V_\alpha)$ ,  $\text{FBH}(V_\alpha)$  and  $\text{CBH}(V_\alpha)$  are reported for the three variational approximations. The variational 95% posterior probability intervals are reported in parentheses.

Figure 1: Comparison of posterior mean estimates of the latent states for the inflation data using different estimators



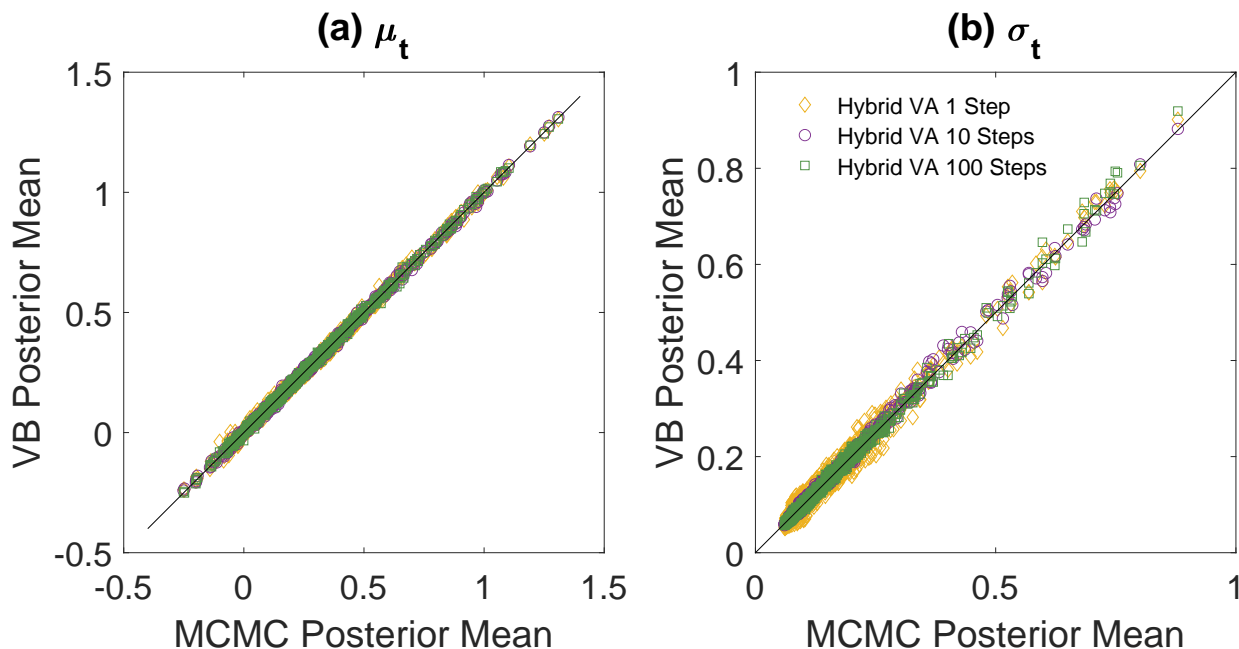
Results are given for  $\mu_t$  in panel (a), and for  $\sigma_t = \exp(\eta_t/2)$  in panel (b), for  $t = 1, \dots, T$ . The exact posterior mean computed by accurate MCMC is plotted in black, that for the VA at (5) in yellow, and that for the structured Gaussian VA in red.

Figure 2: Comparison of posterior estimates for the inflation data using different estimators.



Density estimates are provided on the original parameters of the UCSV mode. Exact estimates computed by accurate MCMC are plotted in black, that for the VA at (5) in yellow, and that for the structured Gaussian VA in red.

Figure 3: Comparison of posterior mean estimates of the latent states for the inflation data using different draws of  $\mathbf{z}$ .



Results are given for  $\mu_t$  in panel (a), and for  $\sigma_t = \exp(\eta_t/2)$  in panel (b), for  $t = 1, \dots, T$ . Each panel plots a scatter of the exact posterior means against the means of the VA at (5) computed using Algorithm 1 with 1, 10 and 100 sweeps of a Gibbs sampler at step (d) of the algorithm.

Figure 4: Comparing the average KL divergence from variational predictives to Bayes exact predictive.

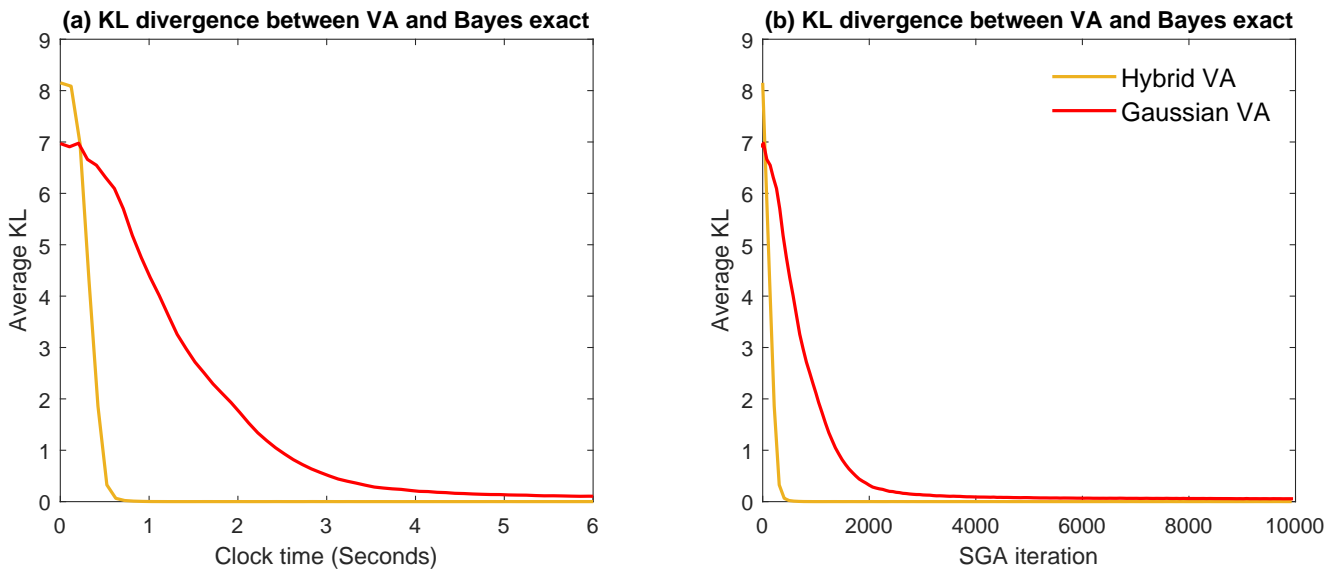
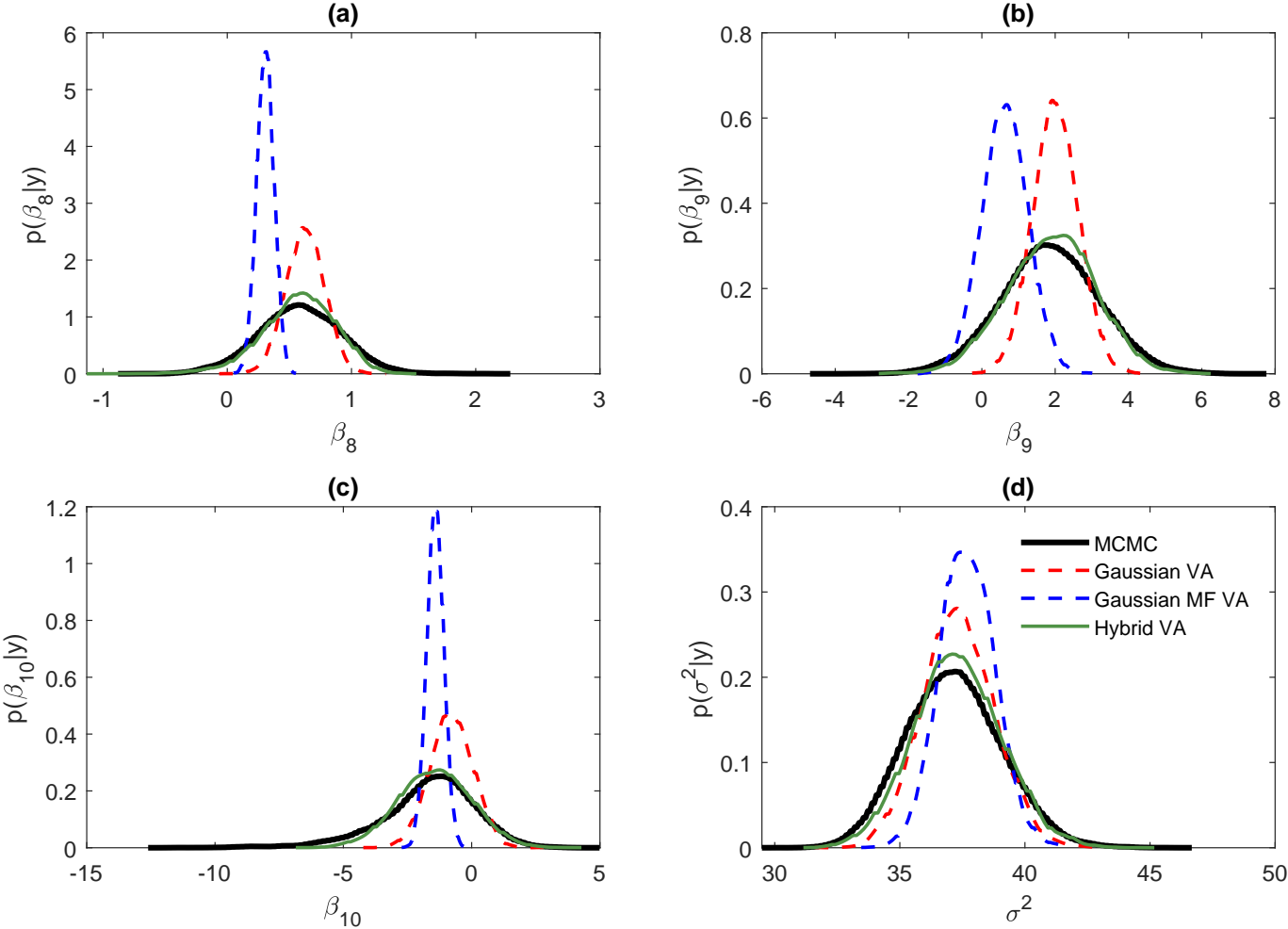
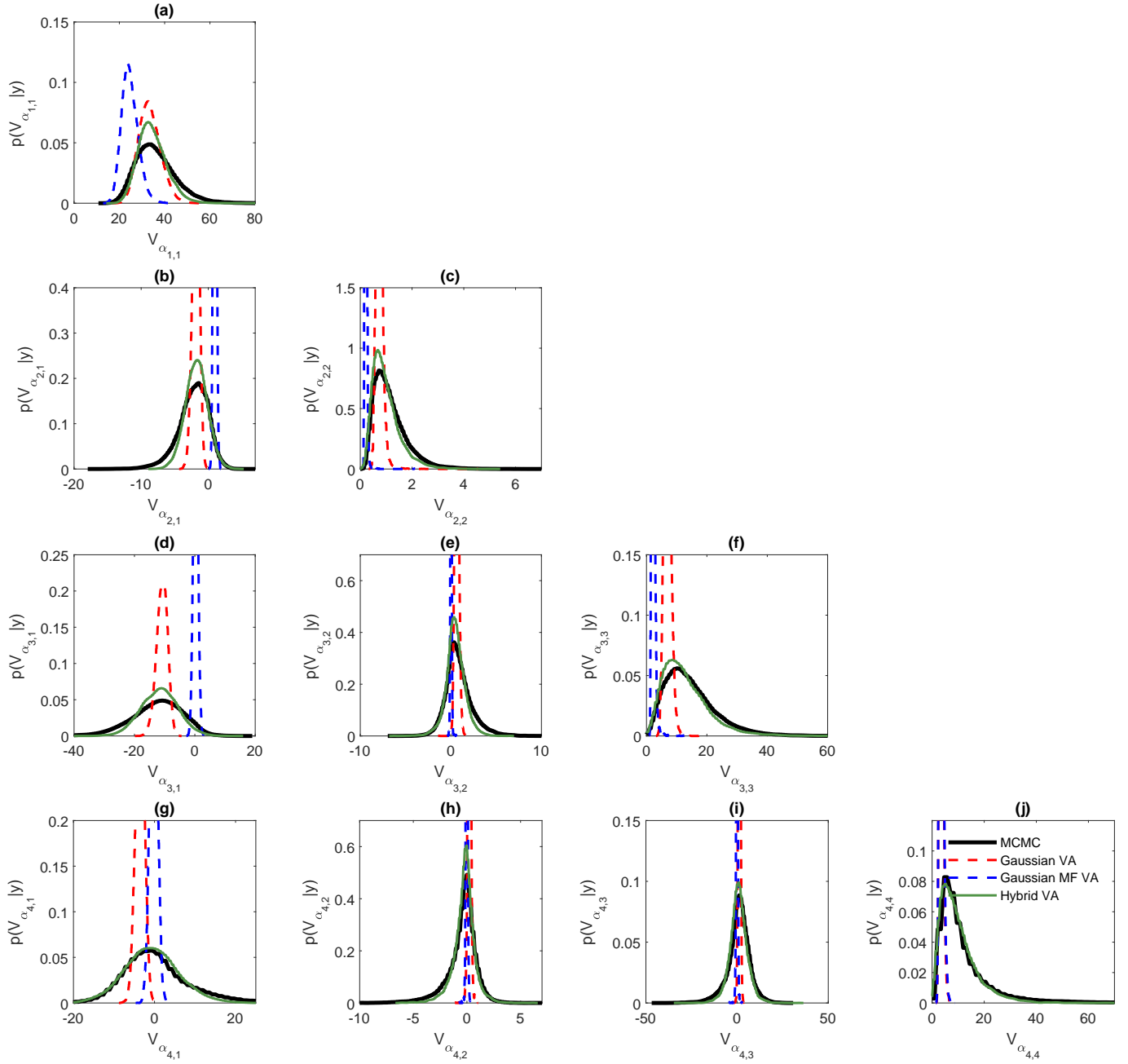


Figure 5: Posterior distributions of select elements of  $\beta$  and  $\sigma^2$  for the small Tobit example.



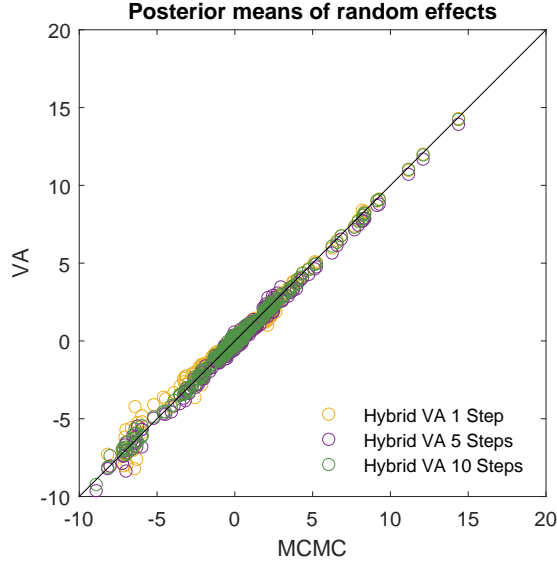
Results are given for (a–c) three select fixed effect coefficients, and (d) the disturbance variance. The black line depicts the exact posteriors computed using MCMC. The blue dashed line depicts the Gaussian Mean Field VA, the red thin dashed line the Gaussian VA, and our proposed estimator as a green thin line.



The panels give the distributions for the lower triangular elements in the  $4 \times 4$  matrix  $V_\alpha$ . The black line depicts the exact posteriors computed using MCMC. The blue dashed line depicts the Gaussian Mean Field VA, the red thin dashed line the Gaussian VA, and our proposed estimator as a green thin line. In panel (j) the two Gaussian VA estimates are so similar they are indistinguishable (i.e. the lines sit on top of one another).

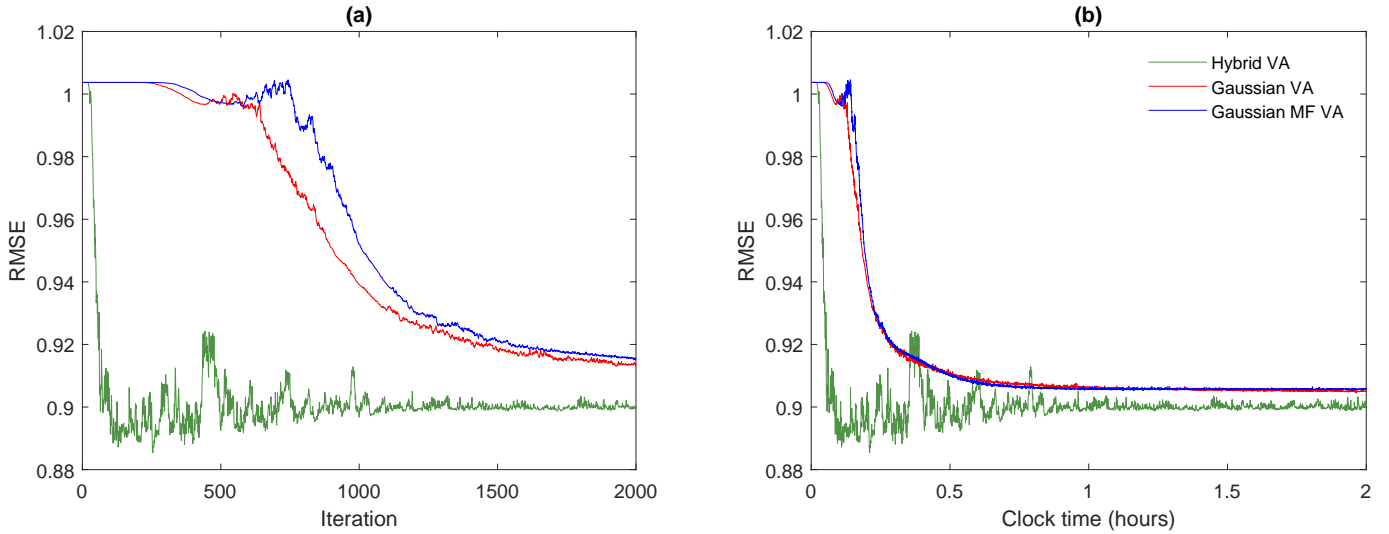


Figure 7: Accuracy of the random coefficient estimates for the small Tobit example.



Scatter-plots of VB mean estimates of the  $Nr = 400$  random coefficients  $\alpha$  against their true posterior means computed using MCMC. Accurate estimates fall on the 45 degree line. Results are given for our proposed VA using 1, 5 and 10 sweeps of a Gibbs sampler at step (d) of Algorithm 1.

Figure 8: Comparison of calibration speed for the full data Tobit example.



Calibration accuracy is measured by the  $\text{RMSE}(\alpha, \theta)$ . This is plotted against both (a) step number, and (b) clock time, for the Gaussian factor (red), mean field Gaussian (blue), and our proposed hybrid (green) variational approximations.

# Online Appendix for ‘Efficient variational inference for models with many latent variables’

This Online Appendix has two parts:

**Part A:** Additional details and results for Section 3.

**Part B:** Additional details and results for Section 4.

## Part A: Additional Details and Results for Section 3

This appendix is split into five sub-sections. Further details on the augmented posterior are given in A.1, and the priors in A.2. The required gradients and derivatives for the SGA algorithm are derived in A.3, while the MCMC scheme used to provide exact posterior estimates is given in A.4. Additional empirical results in A.5.

### A.1 Augmented posterior

The parameters of the UCSV model are  $\boldsymbol{\theta} = (\bar{\mu}, \kappa_\mu, \log(\sigma_\mu^2), \bar{\eta}, \kappa_\eta, \log(\sigma_\eta^2))'$ . By denoting  $c_\mu = \log(\sigma_\mu^2)$  and  $c_\eta = \log(\sigma_\eta^2)$ , we can re-express this parameter vector as  $\boldsymbol{\theta} = (\bar{\mu}, \kappa_\mu, c_\mu, \bar{\eta}, \kappa_\eta, c_\eta)'$ . The augmented posterior can be written as

$$p(\boldsymbol{\theta}, \mathbf{z} | \mathbf{y}) \propto \frac{1}{e^{\frac{\eta_1}{2}} s_\mu s_\eta} \phi_1\left(\frac{y_1 - \mu_1}{e^{\frac{\eta_1}{2}}}\right) \phi_1\left(\frac{\mu_1 - \bar{\mu}}{s_\mu}\right) \phi_1\left(\frac{\eta_1 - \bar{\eta}}{s_\eta}\right) \prod_{t=2}^T \frac{1}{e^{\frac{\eta_t}{2}} \sigma_\mu \sigma_\eta} \phi_1\left(\frac{y_t - \mu_t}{e^{\frac{\eta_t}{2}}}\right) \times \\ \phi_1\left(\frac{\mu_t - \bar{\mu} \rho_\mu (\mu_{t-1} - \bar{\mu})}{\sigma_\mu}\right) \phi_1\left(\frac{\eta_t - \bar{\eta} - \rho_\eta (\eta_{t-1} - \bar{\eta})}{\sigma_\eta}\right) p(\boldsymbol{\theta}),$$

where  $s_\eta^2 = \frac{\sigma_\eta^2}{1 - \rho_\eta^2}$  and  $s_\mu^2 = \frac{\sigma_\mu^2}{1 - \rho_\mu^2}$ . Therefore, a closed-form expression for  $\log g(\boldsymbol{\theta}, \mathbf{z})$  is:

$$\log g(\boldsymbol{\theta}, \mathbf{z}) = \log p(\boldsymbol{\theta}) - \frac{\eta_1}{2} - \log(s_\mu) - \log(s_\eta) - \frac{1}{2} \left(\frac{y_1 - \mu_1}{e^{\frac{\eta_1}{2}}}\right)^2 - \frac{1}{2} \left(\frac{\mu_1 - \bar{\mu}}{s_\mu}\right)^2 - \frac{1}{2} \left(\frac{\eta_1 - \bar{\eta}}{s_\eta}\right)^2 + \\ \sum_{t=2}^T \left[ -\frac{\eta_t}{2} - \log(\sigma_\mu) - \log(\sigma_\eta) - \frac{1}{2} \left(\frac{y_t - \mu_t}{e^{\frac{\eta_t}{2}}}\right)^2 - \frac{1}{2} \left(\frac{\mu_t - \bar{\mu} - \rho_\mu (\mu_{t-1} - \bar{\mu})}{\sigma_\mu}\right)^2 - \right. \\ \left. \frac{1}{2} \left(\frac{\eta_t - \bar{\eta} - \rho_\eta (\eta_{t-1} - \bar{\eta})}{\sigma_\eta}\right)^2 \right].$$

### A.2 Prior choice

The prior is defined as  $p(\boldsymbol{\theta}) = p(\bar{\mu})p(\kappa_\mu)p(c_\mu)p(\bar{\eta})p(\kappa_\eta)p(c_\eta)$ , with

$$\begin{aligned} \text{(i)} \quad p(\bar{\mu}) &= \phi_1(\bar{\mu}; 0, 1000), & \text{(ii)} \quad p(\kappa_\mu) &= \phi_1(\kappa_\mu; 0, 1), & \text{(iii)} \quad p(c_\mu) &\propto e^{-\alpha c_\mu} \exp\left(-\frac{\beta}{e^{c_\mu}}\right) \\ \text{(iv)} \quad p(\bar{\eta}) &= \phi_1(\bar{\eta}; 0, 1000), & \text{(v)} \quad p(\kappa_\eta) &= \phi_1(\kappa_\eta; 0, 1), & \text{(vi)} \quad p(c_\eta) &\propto e^{-\alpha c_\eta} \exp\left(-\frac{\beta}{e^{c_\eta}}\right) \end{aligned}$$

Here,  $p(c_\mu)$  and  $p(c_\eta)$  were constructed by considering an inverse gamma prior on  $\sigma_\mu^2$  and  $\sigma_\eta^2$ , and deriving the corresponding priors on  $c_\mu$  and  $c_\eta$ . The shape and rate parameters of the inverse prior are set as  $\alpha = 1.001$  and  $\beta = 1.001$ . The priors  $p(\kappa_\mu)$  and  $p(\kappa_\eta)$  were constructed by considering a

uniform prior on  $\rho_\mu$  and  $\rho_\eta$ , and deriving the corresponding priors on  $\kappa_\mu$  and  $\kappa_\eta$ .

### A.3 Derivation of gradients

First, note that the derivatives of the priors with respect to their corresponding arguments are:

$$\begin{aligned} \text{(i)} \quad \frac{\partial \log p(\bar{\mu})}{\partial \bar{\mu}} &= -\frac{\bar{\mu}}{1000}, & \text{(ii)} \quad \frac{\partial \log p(\kappa_\mu)}{\partial \kappa_\mu} &= -\kappa_\mu, & \text{(iii)} \quad \frac{\partial \log p(c_\mu)}{\partial c_\mu} &= -\alpha + \beta e^{-c_\mu} \\ \text{(iv)} \quad \frac{\partial \log p(\bar{\eta})}{\partial \bar{\eta}} &= -\frac{\bar{\eta}}{1000}, & \text{(v)} \quad \frac{\partial \log p(\kappa_\eta)}{\partial \kappa_\eta} &= -\kappa_\eta, & \text{(vi)} \quad \frac{\partial \log p(c_\eta)}{\partial c_\eta} &= -\alpha + \beta e^{-c_\eta} \end{aligned}$$

With these derivatives we can then construct

$$\nabla_{\boldsymbol{\theta}} \log g(\boldsymbol{\theta}, \mathbf{z}) = (\nabla_{\bar{\mu}} \log g(\boldsymbol{\psi}), \nabla_{\kappa_\mu} \log g(\boldsymbol{\psi}), \nabla_{c_\mu} \log g(\boldsymbol{\psi}), \nabla_{\bar{\eta}} \log g(\boldsymbol{\psi}), \nabla_{\kappa_\eta} \log g(\boldsymbol{\psi}), \nabla_{c_\eta} \log g(\boldsymbol{\psi}))^\top$$

with each of its elements defined as:

$$\begin{aligned} \nabla_{\bar{\mu}} \log g(\boldsymbol{\psi}) &= \frac{\partial \log p(\bar{\mu})}{\partial \bar{\mu}} + \frac{\mu_1 - \bar{\mu}}{s_\mu^2} - \sum_{t=2}^T \frac{(\rho_\mu - 1)}{\sigma_\mu} \left[ \frac{\mu_t - \bar{\mu} - \rho_\mu(\mu_{t-1} - \bar{\mu})}{\sigma_\mu} \right] \\ \nabla_{\kappa_\mu} \log g(\boldsymbol{\psi}) &= \frac{\partial \log p(\kappa_\mu)}{\partial \kappa_\mu} + \left\{ \frac{\rho_\mu}{1 - \rho_\mu^2} \left[ \frac{(\mu_1 - \bar{\mu})^2}{s_\mu^2} - 1 \right] + \sum_{t=2}^T \frac{\mu_{t-1} - \bar{\mu}}{\sigma_\mu^2} [\mu_t - \bar{\mu} - \rho_\mu(\mu_{t-1} - \bar{\mu})] \right\} \phi_1(\kappa_\mu) R \\ \nabla_{c_\mu} \log g(\boldsymbol{\psi}) &= \frac{\partial \log p(c_\mu)}{\partial c_\mu} - \frac{1}{2} + \frac{(\mu_1 - \bar{\mu})^2}{2s_\mu^2} + \sum_{t=2}^T -\frac{e^{\frac{c_\mu}{2}}}{2\sigma_\mu} + \frac{[\mu_t - \bar{\mu} - \rho_\mu(\mu_{t-1} - \bar{\mu})]^2 e^{\frac{c_\mu}{2}}}{2\sigma_\mu^3} \\ \nabla_{\bar{\eta}} \log g(\boldsymbol{\psi}) &= \frac{\partial \log p(\bar{\eta})}{\partial \bar{\eta}} + \frac{\eta_1 - \bar{\eta}}{s_\eta^2} - \sum_{t=2}^T \frac{(\rho_\eta - 1)}{\sigma_\eta} \left[ \frac{\eta_t - \bar{\eta} - \rho_\eta(\eta_{t-1} - \bar{\eta})}{\sigma_\eta} \right] \\ \nabla_{\kappa_\eta} \log g(\boldsymbol{\psi}) &= \frac{\partial \log p(\kappa_\eta)}{\partial \kappa_\eta} + \left\{ \frac{\rho_\eta}{1 - \rho_\eta^2} \left[ \frac{(\eta_1 - \bar{\eta})^2}{s_\eta^2} - 1 \right] + \sum_{t=2}^T \frac{\eta_{t-1} - \bar{\eta}}{\sigma_\eta^2} [\eta_t - \bar{\eta} - \rho_\eta(\eta_{t-1} - \bar{\eta})] \right\} \phi_1(\kappa_\eta) R \\ \nabla_{c_\eta} \log g(\boldsymbol{\psi}) &= \frac{\partial \log p(c_\eta)}{\partial c_\eta} - \frac{1}{2} + \frac{(\eta_1 - \bar{\eta})^2}{2s_\eta^2} + \sum_{t=2}^T -\frac{e^{\frac{c_\eta}{2}}}{2\sigma_\eta} + \frac{[\eta_t - \bar{\eta} - \rho_\eta(\eta_{t-1} - \bar{\eta})]^2 e^{\frac{c_\eta}{2}}}{2\sigma_\eta^3} \end{aligned}$$

The expression above were computed using the standard chain rule, and the fact that  $\frac{\partial \rho_\eta}{\partial \kappa_\eta} = \phi(\kappa_\eta)R$ ,  $\frac{\partial \rho_\mu}{\partial \kappa_\mu} = \phi(\kappa_\mu)R$ ,  $\frac{\partial \sigma_\eta^2}{\partial c_\eta} = e^{c_\eta}$  and  $\frac{\partial \sigma_\mu^2}{\partial c_\mu} = e^{c_\mu}$ , with  $R = 0.995$ .

## A.4 Exact Bayesian inference

For exact Bayesian inference on the augmented posterior we employ the following MCMC sampling scheme:

### Sampling Scheme

- |  |  |
|--|--|
| Step 1: Generate from $\boldsymbol{\eta} \boldsymbol{\mu}, \boldsymbol{\theta}, \mathbf{y}$ .  | Step 5: Generate from $\bar{\eta} \boldsymbol{\mu}, \boldsymbol{\eta}, \mathbf{y}, \{\boldsymbol{\theta}\setminus\bar{\eta}\}$ .     |
| Step 2: Generate from $\boldsymbol{\mu} \boldsymbol{\eta}, \boldsymbol{\theta}, \mathbf{y}$ .  | Step 6: Generate from $\sigma_\mu^2 \boldsymbol{\mu}, \boldsymbol{\eta}, \mathbf{y}, \{\boldsymbol{\theta}\setminus\sigma_\mu^2\}$ . |
| Step 3: Generate from $\sigma_\eta^2 \boldsymbol{\mu}, \boldsymbol{\eta}, \mathbf{y}, \{\boldsymbol{\theta}\setminus\sigma_\eta^2\}$ . | Step 7: Generate from $\rho_\mu \boldsymbol{\mu}, \boldsymbol{\eta}, \mathbf{y}, \{\boldsymbol{\theta}\setminus\rho_\mu^2\}$ .       |
| Step 4: Generate from $\rho_\eta \boldsymbol{\mu}, \boldsymbol{\eta}, \mathbf{y}, \{\boldsymbol{\theta}\setminus\rho_\eta\}$ .         | Step 8: Generate from $\bar{\mu} \boldsymbol{\mu}, \boldsymbol{\eta}, \mathbf{y}, \{\boldsymbol{\theta}\setminus\bar{\mu}\}$ .       |

For Step 1, we proceed as in Primiceri (2005), using a mixture of seven normals to approximate the distribution of  $\log [(y_t - \mu_t)^2 e^{-2\eta t}]$ , and then the precision sampler in Chan and Jeliazkov (2009) to generate  $\boldsymbol{\eta}$ . The precision sampler is also used to generate  $\boldsymbol{\mu}$  in Step 2. For steps 3 and 6 we use the inverse gamma distributions:

$$p(\sigma_\eta^2|\boldsymbol{\mu}, \boldsymbol{\eta}, \mathbf{y}, \{\boldsymbol{\theta}\setminus\sigma_\eta^2\}) = \text{IG} \left( \alpha + \frac{T}{2}, \beta + \frac{1}{2} \left[ (\eta_1 - \bar{\eta})^2 (1 - \rho_\eta^2) + \sum_{t=2}^T (\eta_t - \rho_\eta \eta_{t-1} - \bar{\eta} (1 - \rho_\eta))^2 \right] \right)$$

$$p(\sigma_\mu^2|\boldsymbol{\mu}, \boldsymbol{\eta}, \mathbf{y}, \{\boldsymbol{\theta}\setminus\sigma_\mu^2\}) = \text{IG} \left( \alpha + \frac{T}{2}, \beta + \frac{1}{2} \left[ (\mu_1 - \bar{\mu})^2 (1 - \rho_\mu^2) + \sum_{t=2}^T (\mu_t - \rho_\mu \mu_{t-1} - \bar{\mu} (1 - \rho_\mu))^2 \right] \right)$$

In steps 5 and 8 we use the Gaussian distributions:

$$p(\bar{\eta}|\boldsymbol{\mu}, \boldsymbol{\eta}, \mathbf{y}, \{\boldsymbol{\theta}\setminus\bar{\eta}\}) = \text{N}(\mu_{\bar{\eta}}, s_{\bar{\eta}}^2) \quad \text{and} \quad p(\bar{\mu}|\boldsymbol{\mu}, \boldsymbol{\eta}, \mathbf{y}, \{\boldsymbol{\theta}\setminus\bar{\mu}\}) = \text{N}(\mu_{\bar{\mu}}, s_{\bar{\mu}}^2)$$

$$\text{with } s_{\bar{\eta}}^2 = \left[ \frac{1}{1000} + \frac{(T-1)(1-\rho_\eta)^2 + (1-\rho_\eta^2)}{\sigma_\eta^2} \right]^{-1}, \quad \mu_{\bar{\eta}} = s_{\bar{\eta}}^2 \left[ \frac{(1-\rho_\eta^2)\eta_1}{\sigma_\eta^2} + \frac{(1-\rho_\eta)}{\sigma_\eta^2} \sum_{t=2}^T (\eta_t - \rho_\eta \eta_{t-1}) \right],$$

$$s_{\bar{\mu}}^2 = \left[ \frac{1}{1000} + \frac{(T-1)(1-\rho_\mu)^2 + (1-\rho_\mu^2)}{\sigma_\mu^2} \right]^{-1} \quad \text{and} \quad \mu_{\bar{\mu}} = s_{\bar{\mu}}^2 \left[ \frac{(1-\rho_\mu^2)\mu_1}{\sigma_\mu^2} + \frac{(1-\rho_\mu)}{\sigma_\mu^2} \sum_{t=2}^T (\mu_t - \rho_\mu \mu_{t-1}) \right].$$

In steps 4 and 7 we use a Metropolis Hastings step, with corresponding proposals

$$p(\rho_\eta) = \text{N}(\mu_{\rho_\eta}, s_{\rho_\eta}^2) \quad \text{and} \quad p(\rho_\mu) = \text{N}(\mu_{\rho_\mu}, s_{\rho_\mu}^2)$$

where  $s_{\rho_\eta}^2 = \sigma_\eta^2 \left[ \sum_{t=1}^{T-1} (\eta_t - \bar{\eta})^2 \right]^{-1}$ ,  $\mu_{\rho_\eta} = s_{\rho_\eta}^2 \frac{\sum_{t=2}^T (\eta_t - \bar{\eta})(\eta_{t-1} - \bar{\eta})}{\sigma_\eta^2}$ ,  $s_{\rho_\mu}^2 = \sigma_\mu^2 \left[ \sum_{t=1}^{T-1} (\mu_t - \bar{\mu})^2 \right]^{-1}$  and  $\mu_{\rho_\mu} = s_{\rho_\mu}^2 \frac{\sum_{t=2}^T (\mu_t - \bar{\mu})(\mu_{t-1} - \bar{\mu})}{\sigma_\mu^2}$ . Note here that steps 1 and 2 in this sampling scheme can also be employed to generate from  $p(\boldsymbol{\eta}|\mathbf{y}, \boldsymbol{\theta}^{(s)}, \boldsymbol{\mu}^{(s)})$  and  $p(\boldsymbol{\mu}|\mathbf{y}, \boldsymbol{\theta}^{(s)}, \boldsymbol{\eta}^{(s-1)})$  in the hybrid variational approximation algorithm.

**Additional References**

Carter, C. and Kohn, R. (1994). On Gibbs sampling for state space models. *Biometrika*, 81(3): 541-553.

Primiceri, G. (2005). Time Varying Structural Vector Autoregressions and Monetary Policy. *Review of Economic Studies*. 72(3): 821-852.

**A.5 Supplemental figures**

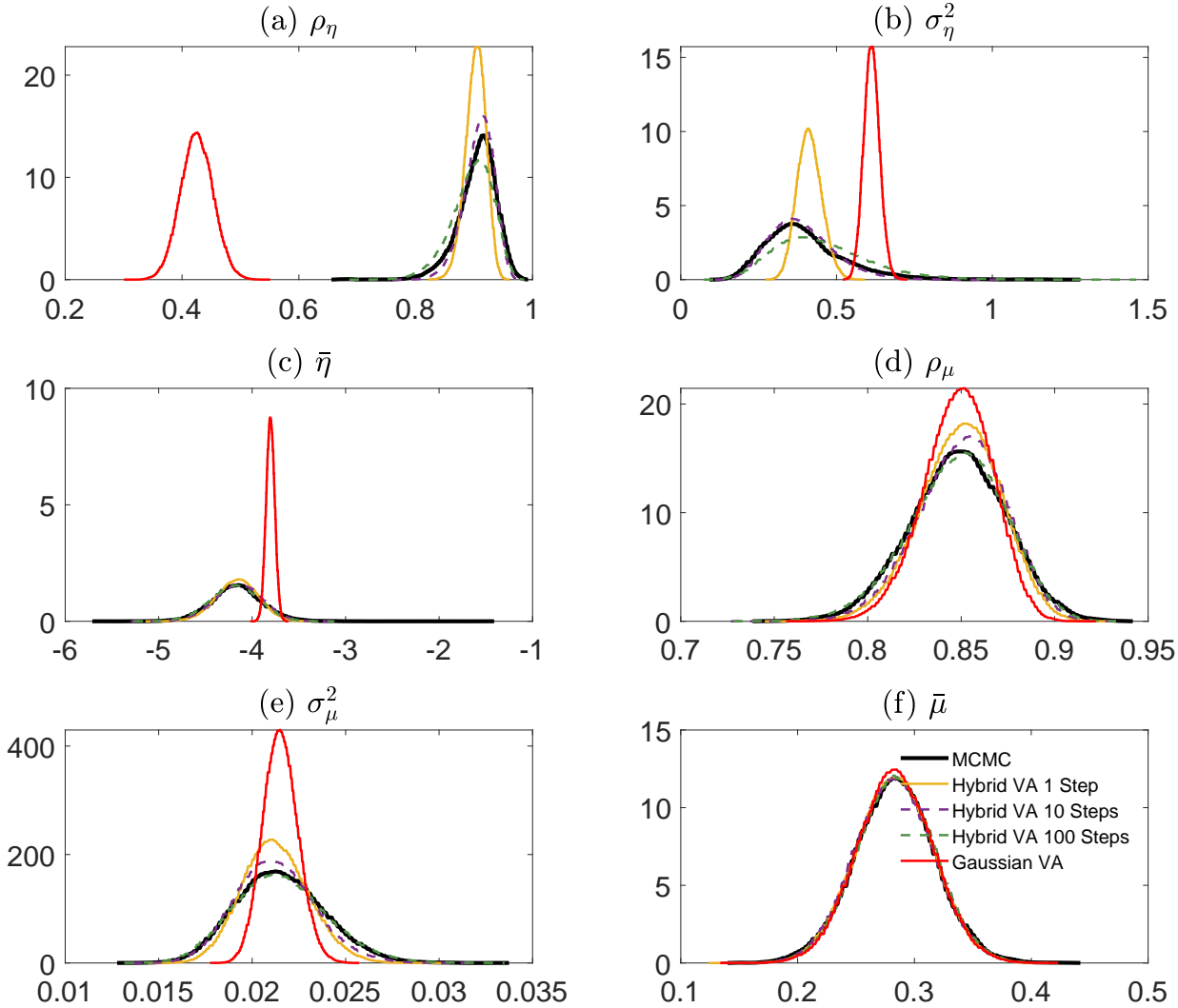


Figure 1: Estimated posterior distribution of the global model parameters of the UCSV model fit to the U.S. inflation time series. The exact posterior is given in black, the structured Gaussian VA is given in red, while our proposed Hybrid VA with 1, 10 and 100 sweeps at step (d) of Algorithm 1 are also given.

## Part B: Additional Details and Results for Section 4

This appendix is split in five sub-sections. Sub-section B.1 provides further details on the augmented posterior. In B.2 the prior choices for the parameters of the model are outlined. In sub-section B.3 all the required gradients and derivatives for the SGA algorithm are derived. Sub-section B.4 provides details on MCMC estimation of the tobit model. Finally, B.5 provides supplemental results for the empirical application.

### B.1 Augmented posterior

The parameters of the mixed effects tobit model are  $\boldsymbol{\theta} = (\boldsymbol{\beta}^\top, \text{vech}(L)^\top, \boldsymbol{\omega}^\top, \sigma^2)^\top$ . All the elements in  $\boldsymbol{\theta}$  need to be transformed to the real line. To do this, we introduce  $c = \log(1/\sigma)$ ,  $\xi_i = \log(\omega_i)$ ,  $\boldsymbol{\xi} = (\xi_1, \dots, \xi_r)^\top$ ,  $\kappa_j = \log(L_{j,j})$ ,  $\boldsymbol{\kappa} = (\kappa_1, \dots, \kappa_{k_\alpha})^\top$ , and  $\boldsymbol{l}$  which denotes the elements in  $\text{vech}(L)$  with the diagonal elements of  $L$  excepted. We then re-express this parameter vector as  $\boldsymbol{\theta} = (\boldsymbol{\beta}^\top, \boldsymbol{\xi}^\top, c, \boldsymbol{\kappa}^\top, \boldsymbol{l}^\top)^\top$ . Given this parameter transformation, the augmented posterior can be written as

$$p(\mathbf{y}^*, \boldsymbol{\alpha}, \boldsymbol{\theta} | \mathbf{y}) = \left[ \prod_{i=1, t=1}^{N, T} \phi_1(y_{it}^*; \eta_{it}, \sigma^2) \right] \left[ \prod_{i=1}^N \phi_r(\boldsymbol{\alpha}_i; \mathbf{0}, V_\alpha) \right] p(\boldsymbol{\theta})$$

### B.2 Prior choice

The prior is defined as  $p(\boldsymbol{\theta}) = p(\boldsymbol{\beta}) p(\boldsymbol{\xi}) p(c) p(\boldsymbol{\kappa}) p(\boldsymbol{l})$ , with

$$\begin{aligned} \text{(i)} \quad p(\boldsymbol{\beta}) &= \phi_p(\boldsymbol{\beta}; \mathbf{0}, \Sigma_\beta), & \text{(ii)} \quad p(\boldsymbol{\xi}) &= \prod_{i=1}^r \exp(\xi_i)^{-1} \exp\left(-\frac{1}{\exp(\xi_i)}\right), & \text{(iii)} \quad p(c) &\propto 1 \\ \text{(iv)} \quad p(\boldsymbol{\kappa}) &= \prod_{j=1}^{k_\alpha} 2\phi_1(\exp(\kappa_j); 0, \sigma_l^2) \exp(\kappa_j), & \text{(v)} \quad p(\boldsymbol{l}) &= \prod_{i=2}^r \prod_{j=1}^{\min(i-1, k_\alpha)} \phi_1(L_{i,j}; 0, \sigma_l^2), \end{aligned}$$

Here,  $p(c)$  was constructed by considering the prior  $p(\sigma^2) \propto \frac{1}{\sigma^2}$  and deriving the corresponding prior on  $c$ . The prior  $p(\boldsymbol{\xi})$  was constructed by using the prior  $p(\boldsymbol{\omega}) = \prod_{i=1}^r p(\omega_i)$ , with  $p_\omega(\omega_i) = \text{Inv-Gamma}(\omega_i, 1, 1)$ , and then using the Jacobian of the transformation to derive the corresponding prior on  $\boldsymbol{\xi}$ . Finally,  $p(\boldsymbol{\kappa})$  was constructed by considering the truncated normal prior  $2\phi_1(L_{j,j}; 0, \sigma_l^2) I(L_{j,j} > 0)$  on  $L_{j,j}$  and deriving the corresponding prior for  $\kappa_j$  via the Jacobian of the transformation.

### B.3 Computing gradients

Given the expressions for the augmented posterior and prior densities above, the function  $\log g(\boldsymbol{\theta}, \mathbf{z})$  can be written as:

$$\begin{aligned}
\log g(\boldsymbol{\theta}, \mathbf{z}) &= \log \left\{ \left[ \prod_{i=1, t=1}^{N, T} \phi_1(y_{it}^*; \eta_{it}, \sigma^2) \right] \left[ \prod_{i=1}^N \phi_r(\boldsymbol{\alpha}_i; \mathbf{0}, V_\alpha) \right] p(\boldsymbol{\beta}) p(\boldsymbol{\xi}) p(c) p(\boldsymbol{\kappa}) p(\mathbf{l}) \right\} \\
&= -\frac{n \log(2\pi)}{2} + nc - \frac{e^{2c}}{2} \sum_{it} (y_{it}^* - \eta_{it})^2 - \frac{rN \log(2\pi)}{2} - \frac{N}{2} \log(|V_\alpha|) - \\
&\quad \frac{1}{2} \sum_i \boldsymbol{\alpha}_j^\top V_\alpha^{-1} \boldsymbol{\alpha}_j - \frac{p \log(2\pi)}{2} - \frac{1}{2} \log(|\Sigma_\beta|) - \frac{1}{2} \boldsymbol{\beta}^\top \Sigma_\beta^{-1} \boldsymbol{\beta} - \frac{1}{2} r k_\alpha \log(2\pi) - \\
&\quad \frac{r k_\alpha - (k_\alpha - 1) k_\alpha}{2} \log(\sigma_l^2) + k_\alpha \log(2) - \sum_{i=1}^r \sum_{j=1}^{k_\alpha} \frac{l_{i,j}^2}{2\sigma_l^2} + \sum_{j=1}^{k_\alpha} \kappa_j - \sum_{i=1}^r \left( \xi_i + \frac{1}{\exp(\xi_i)} \right) \\
&= \text{const} + nc - \frac{e^{2c}}{2} \sum_{it} (y_{it}^* - \eta_{it})^2 - \frac{N}{2} \log(|V_\alpha|) - \frac{1}{2} \sum_i (\boldsymbol{\alpha}_i^\top \otimes \boldsymbol{\alpha}_i^\top) \text{vec}(V_\alpha^{-1}) - \\
&\quad \frac{1}{2} \boldsymbol{\beta}^\top \Sigma_\beta^{-1} \boldsymbol{\beta} - \sum_{i=1}^r \sum_{j=1}^{k_\alpha} \frac{l_{i,j}^2}{2\sigma_l^2} + \sum_{j=1}^{k_\alpha} \kappa_j - \sum_{i=1}^r \left( \xi_i + \frac{1}{\exp(\xi_i)} \right) \\
&= \text{const} + f(\mathbf{y}^*, \boldsymbol{\alpha}, \boldsymbol{\theta}) + \sum_{j=1}^{k_\alpha} \kappa_j
\end{aligned}$$

The required gradients with respect to  $c$  and  $\boldsymbol{\beta}$  can be computed as:

$$\begin{aligned}
\nabla_c \log g(\boldsymbol{\theta}, \mathbf{z}) &= n - e^{2c} \sum_{it} (y_{it}^* - \eta_{it})^2 \\
\nabla_{\boldsymbol{\beta}} \log g(\boldsymbol{\theta}, \mathbf{z}) &= e^{2c} \sum_{it} (y_{it}^* - \eta_{it}) \mathbf{x}_{it}^\top - \boldsymbol{\beta}^\top \Sigma_\beta^{-1}
\end{aligned}$$

To construct the gradients with respect to  $\mathbf{l}$  and  $\boldsymbol{\kappa}$ , we must first compute

$$\begin{aligned}
\nabla_L f(\mathbf{y}^*, \boldsymbol{\alpha}, \boldsymbol{\theta}) &= -\frac{N}{2} \frac{1}{|V_\alpha|} \frac{\partial |V_\alpha|}{\partial V_\alpha} \frac{\partial V_\alpha}{\partial L} - \frac{1}{2} \sum_i (\boldsymbol{\alpha}_i^\top \otimes \boldsymbol{\alpha}_i^\top) \frac{\partial V_\alpha^{-1}}{\partial V_\alpha} \frac{\partial V_\alpha}{\partial L} - \frac{1}{\sigma_l^2} \text{vec}(L)^\top \\
&= -\frac{N}{2|V_\alpha|} \text{vec}(|V_\alpha| V_\alpha^{-1})^\top \frac{\partial V_\alpha}{\partial L} - \frac{1}{2} \sum_i (\boldsymbol{\alpha}_i^\top \otimes \boldsymbol{\alpha}_i^\top) \frac{\partial V_\alpha^{-1}}{\partial V_\alpha} \frac{\partial V_\alpha}{\partial L} - \frac{1}{\sigma_l^2} \text{vec}(L)^\top
\end{aligned}$$

The elements of the gradients  $\nabla_l f(\mathbf{y}^*, \boldsymbol{\alpha}, \boldsymbol{\theta})$  and  $\nabla_{\boldsymbol{\kappa}} f(\mathbf{y}^*, \boldsymbol{\alpha}, \boldsymbol{\theta})$  can then be constructed using

$$\begin{aligned}
\nabla_{L_{j,i}} \log g(\boldsymbol{\theta}, \mathbf{z}) &= \nabla_{L_{j,i}} f(\mathbf{y}^*, \boldsymbol{\alpha}, \boldsymbol{\theta}) \\
\nabla_{\kappa_j} \log g(\boldsymbol{\theta}, \mathbf{z}) &= \nabla_{L_{j,j}} f(\mathbf{y}^*, \boldsymbol{\alpha}, \boldsymbol{\theta}) \exp(\kappa_j) + 1
\end{aligned}$$



Finally, the gradient with respect to  $\boldsymbol{\xi}$  can be constructed as:

$$\begin{aligned}\nabla_{\boldsymbol{\xi}} \log g(\boldsymbol{\theta}, \mathbf{z}) &= -\frac{N}{2} \frac{1}{|V_{\alpha}|} \frac{\partial |V_{\alpha}|}{\partial V_{\alpha}} \frac{\partial V_{\alpha}}{\partial \boldsymbol{\omega}} \frac{\partial \boldsymbol{\omega}}{\partial \boldsymbol{\xi}} - \frac{1}{2} \sum_i (\boldsymbol{\alpha}_i^{\top} \otimes \boldsymbol{\alpha}_i^{\top}) \frac{\partial V_{\alpha}^{-1}}{\partial V_{\alpha}} \frac{\partial V_{\alpha}}{\partial \boldsymbol{\omega}} \frac{\partial \boldsymbol{\omega}}{\partial \boldsymbol{\xi}} - (\mathbf{1}_r - \boldsymbol{\omega}^{-1}) \\ &= -\frac{N}{2|V_{\alpha}|} \text{vec}(|V_{\alpha}|V_{\alpha}^{-1})^{\top} \frac{\partial V_{\alpha}}{\partial \boldsymbol{\omega}} \frac{\partial \boldsymbol{\omega}}{\partial \boldsymbol{\xi}} - \frac{1}{2} \sum_i (\boldsymbol{\alpha}_i^{\top} \otimes \boldsymbol{\alpha}_i^{\top}) \frac{\partial V_{\alpha}^{-1}}{\partial V_{\alpha}} \frac{\partial V_{\alpha}}{\partial \boldsymbol{\omega}} \frac{\partial \boldsymbol{\omega}}{\partial \boldsymbol{\xi}} - (\mathbf{1}_r - \boldsymbol{\omega}^{-1})\end{aligned}$$

All the expression above can be computed by noting that  $\frac{\partial V_{\alpha}}{\partial L} = (I_{r^2} + K_{r,r})(L \otimes I_r)$  and  $\frac{\partial V_{\alpha}^{-1}}{\partial V_{\alpha}} = -(V_{\alpha}^{-1} \otimes V_{\alpha}^{-1})$ . We can further simplify  $\frac{\partial V_{\alpha}^{-1}}{\partial V_{\alpha}} \frac{\partial V_{\alpha}}{\partial L} = -(I_{r^2} + K_{r,r})(V_{\alpha}^{-1}L \otimes V_{\alpha}^{-1})$ . For the gradients with respect to  $\boldsymbol{\xi}$  we can use  $\frac{\partial V_{\alpha}}{\partial \boldsymbol{\omega}} = I_{r^2}P$ , where  $P$  is the matrix of ones and zeros that extract columns 1,  $r + 2$ ,  $2r + 3, \dots, r^2$ , and  $\frac{\partial \boldsymbol{\omega}}{\partial \boldsymbol{\xi}} = \Omega$ .

## B.4 Exact Bayesian inference

For exact Bayesian inference on the augmented posterior we employ the following MCMC sampling scheme:

### Sampling Scheme

Step 1: Generate from  $\boldsymbol{\alpha}|\mathbf{y}^*, \boldsymbol{\theta}, \mathbf{y}$ .

Step 2: Generate from  $\mathbf{y}^*|\boldsymbol{\alpha}, \boldsymbol{\theta}, \mathbf{y}$ .

Step 3: Generate from  $\boldsymbol{\theta}|\mathbf{y}^*, \boldsymbol{\alpha}, \mathbf{y}$ .

To perform Step 1, note that  $p(\boldsymbol{\alpha}|\mathbf{y}^*, \boldsymbol{\theta}, \mathbf{y}) = \prod_{i=1}^N p(\boldsymbol{\alpha}_i|\mathbf{y}, \mathbf{y}^*, \boldsymbol{\beta})$ , where each density in the product is an  $r$ -dimensional Gaussian density, so that  $p(\boldsymbol{\alpha}_i|\mathbf{y}, \mathbf{y}^*, \boldsymbol{\beta}) = \phi_r(\boldsymbol{\alpha}_i; A_i^{-1}M_i^{\top}, A_i^{-1})$  with  $M_i = \frac{1}{\sigma^2} \sum_{t=1}^T (y_{it}^* - \mathbf{x}_{it}^{\top}\boldsymbol{\beta}) \mathbf{w}_{it}^{\top}$  and  $A_i = V_{\alpha}^{-1} + \frac{1}{\sigma^2} \sum_{t=1}^T \mathbf{w}_{it} \mathbf{w}_{it}^{\top}$ . In Step 2 we draw from  $p(\mathbf{y}^*|\boldsymbol{\alpha}, \boldsymbol{\theta}, \mathbf{y}) = \prod_{it} p(y_{it}^*|y_{it}, \boldsymbol{\alpha}, \boldsymbol{\theta})$ , with

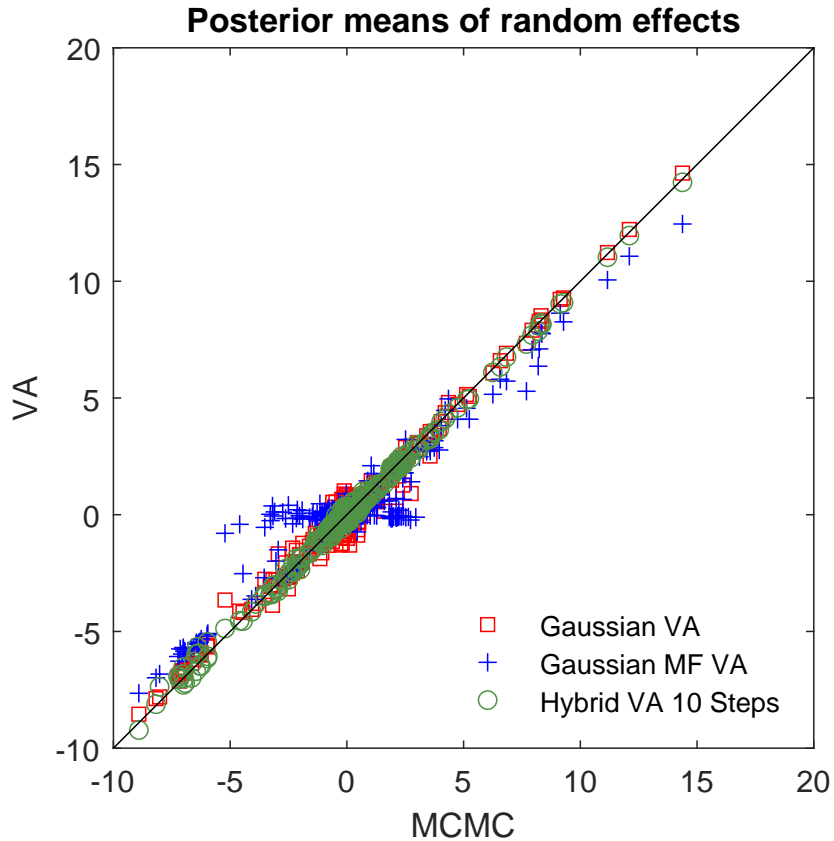
$$p(y_{it}^*|y_{it}, \boldsymbol{\alpha}, \boldsymbol{\theta}) = \begin{cases} \frac{\phi_1(y_{it}^*; \eta_{it}, \sigma^2)}{\Phi_1(0; \eta_{it}, \sigma^2)} I(y_{it}^* \leq 0) & \text{for } y_{it}^* \leq 0 \\ I[y_{ij}^* = y_{it}] & \text{for } y_{it}^* > 0. \end{cases}$$

In Step 3, generation is conducted via random walk Metropolis-Hastings. At the beginning of each iteration, the elements of  $\boldsymbol{\theta}$  are randomly assigned to groups of 10 elements. The groups are then sampled, one group conditional on the other, with the 10-dimensional proposal density equal to the product of 10 independent univariate normals. The variances of the univariate normals are set adaptively to target acceptance rates between 10% and 20%. Note here that steps 1 and 2 in this

sampling scheme can also be employed to generate from  $p(\boldsymbol{\alpha} | (\mathbf{y}^*)^{(s-1)}, \boldsymbol{\theta}^{(s)}, \mathbf{y})$  and  $p(y^* | \boldsymbol{\alpha}^{(s)}, \boldsymbol{\theta}^{(s)}, \mathbf{y})$  in the hybrid variational approximation algorithm.

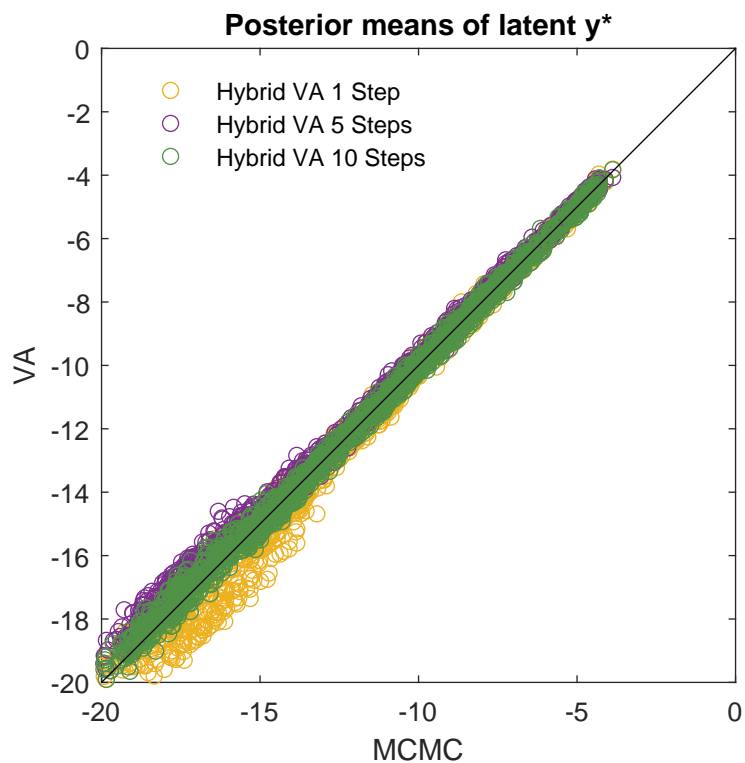
## B.5 Supplemental figures and tables

Figure 2: Accuracy of the random coefficient estimates for the tobit small data example.

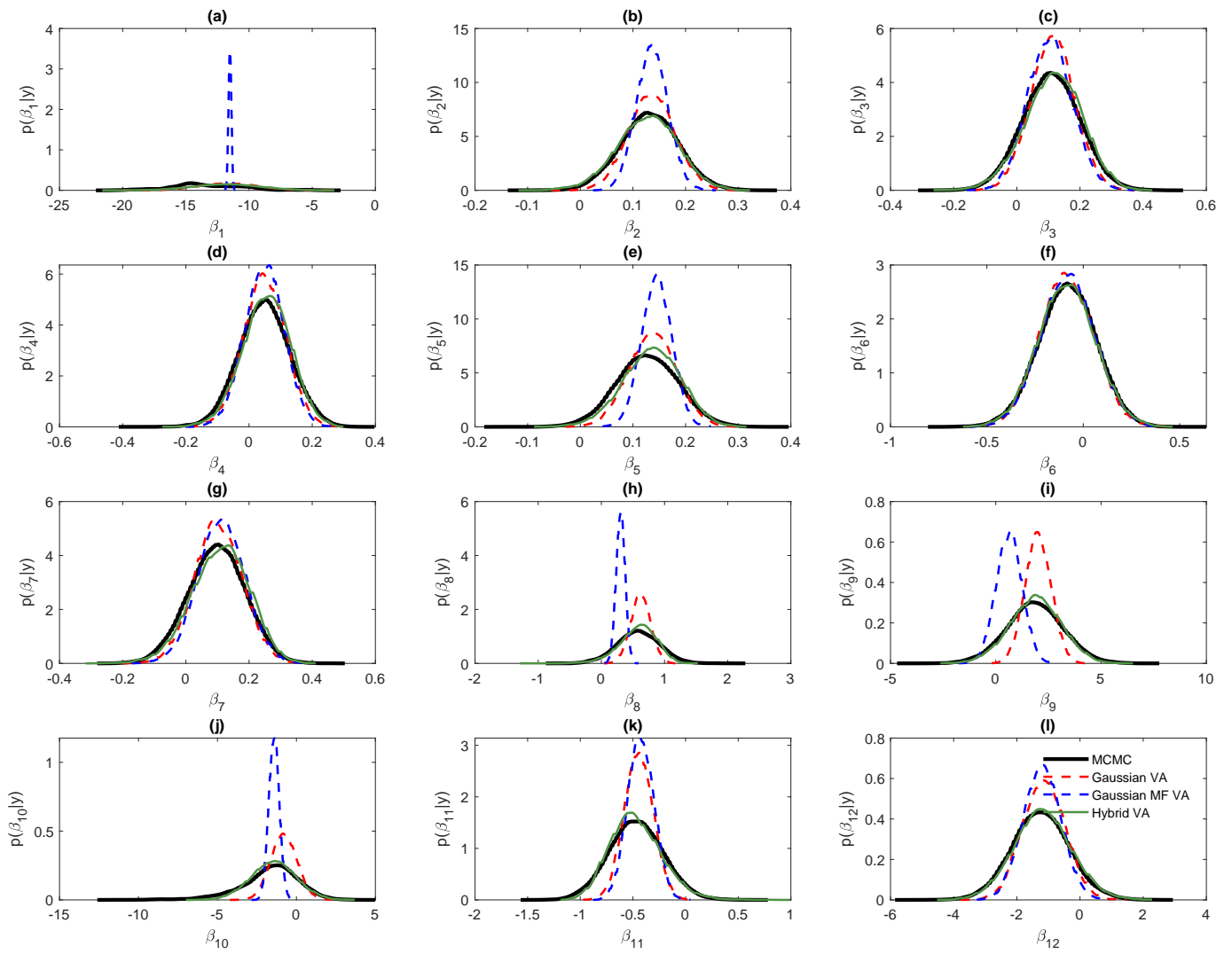


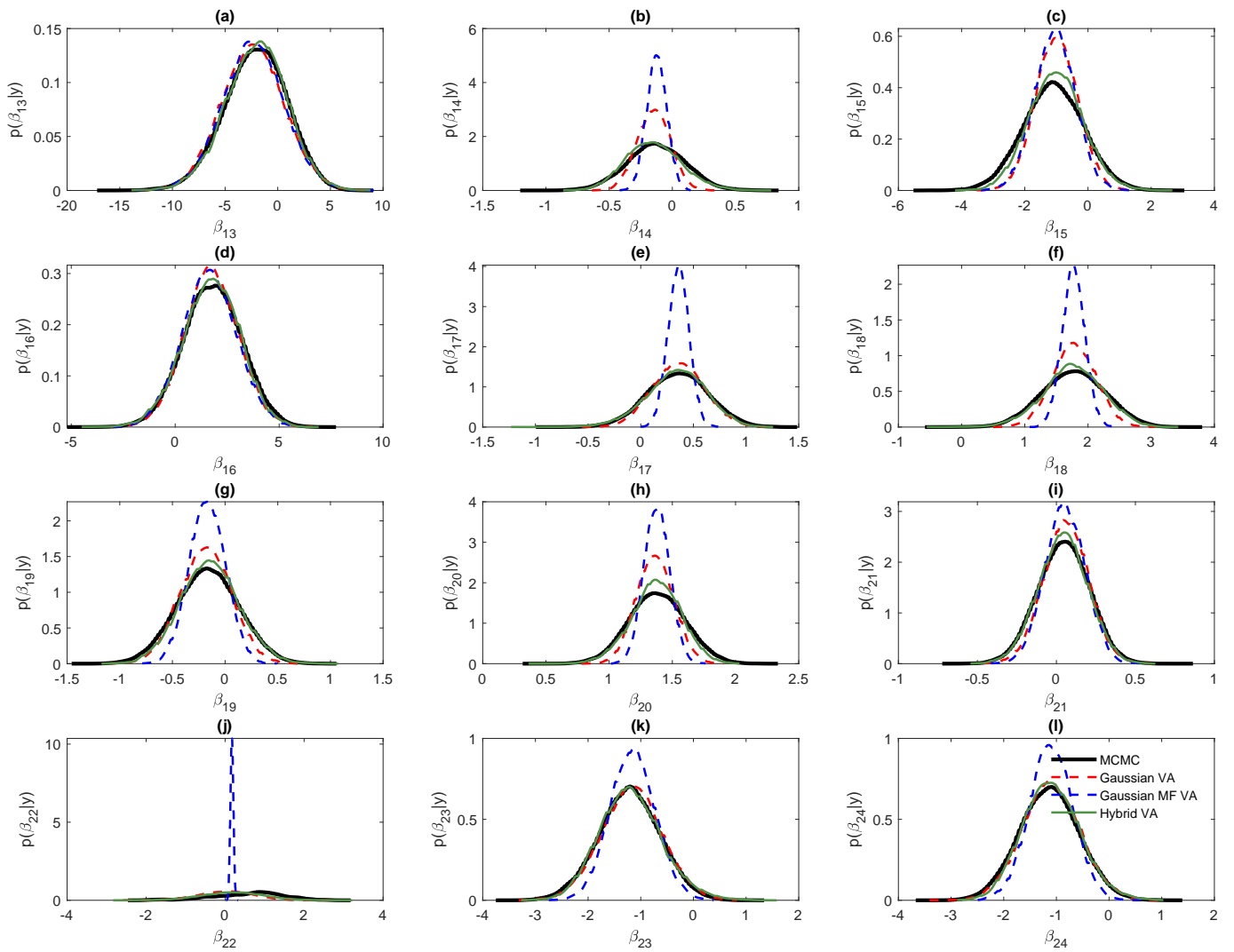
Scatter-plots of VB mean estimates of the  $Nr = 400$  random coefficients  $\boldsymbol{\alpha}$  against their true posterior means computed using MCMC. Accurate estimates fall on the 45 degree line. Results are given for the Gaussian mean field approximation, the Gaussian approximation with factor structure, and our proposed VA using 10 sweeps of a Gibbs sampler at step (d) of Algorithm 1.

Figure 3: Accuracy of the latent  $\mathbf{y}^*$  estimates for the tobit small data example.



Scatter-plots of VB mean estimates of the latent  $\mathbf{y}^*$  values against their true posterior means computed using MCMC. Accurate estimates fall on the 45 degree line. Results are given for the our proposed VA using 1, 5 and 10 sweeps of a Gibbs sampler at step (d) of Algorithm 1.





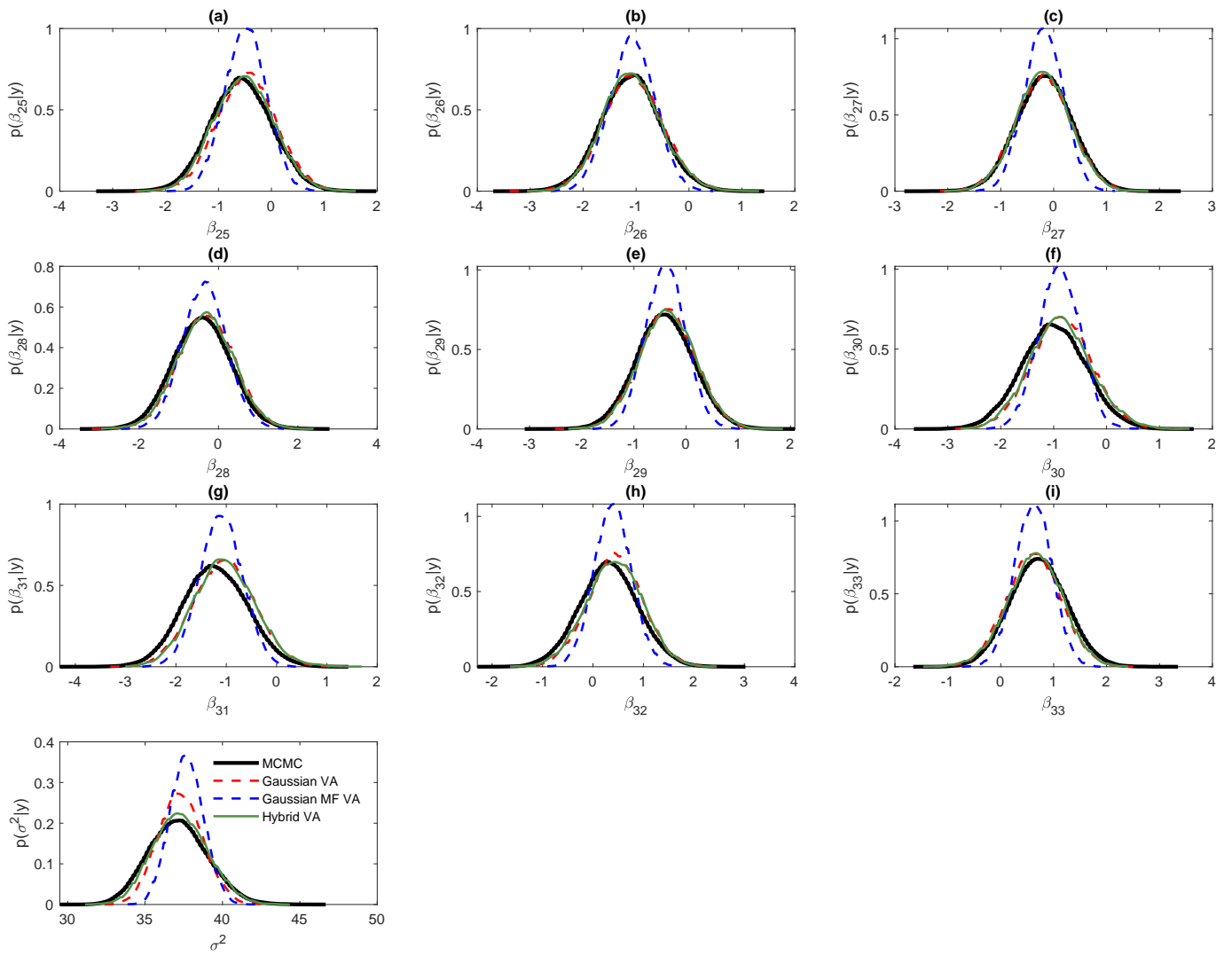


Table A1: Estimate of  $V_\alpha$  for the tobit small data example for MCMC, Hybrid VA and Gaussian factor VA.

	Panel A: MCMC				Panel B: Gaussian VA				
	Intercept	Emails	Catal.	Paid S.	Intercept	Emails	Catal.	Paid S.	
Intercept	35.965 <i>(21.96, 56.14)</i>				Intercept	33.554 <i>(25.03, 44.13)</i>			
Emails	-0.31 <i>(-0.75, 0.31)</i>	1.144 <i>(0.34, 2.79)</i>			Emails	-0.374 <i>(-0.53, -0.20)</i>	0.737 <i>(0.53, 1.04)</i>		
Catal.	-0.536 <i>(-0.92, 0.13)</i>	0.195 <i>(-0.46, 0.72)</i>	14.445 <i>(2.80, 35.39)</i>		Catal.	-0.714 <i>(-0.81, -0.59)</i>	0.292 <i>(0.13, 0.44)</i>	6.977 <i>(4.97, 9.47)</i>	
Paid S.	-0.043 <i>(-0.76, 0.69)</i>	-0.085 <i>(-0.70, 0.54)</i>	0.125 <i>(-0.75, 0.85)</i>	11.749 <i>(1.84, 44.45)</i>	Paid S.	-0.335 <i>(-0.50, -0.15)</i>	0.136 <i>(-0.01, 0.28)</i>	0.254 <i>(0.05, 0.43)</i>	3.495 <i>(2.42, 5.05)</i>
	Panel C: Gaussian MF VA				Panel D: Hybrid VA				
	Intercept	Emails	Catal.	Paid S.	Intercept	Emails	Catal.	Paid S.	
Intercept	24.647 <i>(18.35, 32.54)</i>				Intercept	35.875 <i>(25.52, 48.83)</i>			
Emails	0.435 <i>(0.28, 0.58)</i>	0.208 <i>(0.15, 0.28)</i>			Emails	-0.306 <i>(-0.74, 0.31)</i>	0.985 <i>(0.34, 2.15)</i>		
Catal.	0.04 <i>(-0.16, 0.23)</i>	0.023 <i>(-0.11, 0.15)</i>	2.143 <i>(1.45, 3.25)</i>		Catal.	-0.61 <i>(-0.94, 0.04)</i>	0.173 <i>(-0.42, 0.65)</i>	13.605 <i>(2.51, 34.31)</i>	
Paid S.	-0.022 <i>(-0.22, 0.18)</i>	-0.011 <i>(-0.14, 0.12)</i>	-0.004 <i>(-0.21, 0.2)</i>	3.525 <i>(2.39, 5.23)</i>	Paid S.	-0.08 <i>(-0.77, 0.66)</i>	0.004 <i>(-0.56, 0.57)</i>	0.115 <i>(-0.72, 0.82)</i>	9.986 <i>(1.55, 29.48)</i>

The diagonal values are estimates of the variances of the random coefficients (i.e. the leading diagonal of  $V_\alpha$ ). The off-diagonal values are estimates of the correlations between the random coefficients (i.e. the correlations of the matrix  $V_\alpha$ ). The variational means are reported, along with the 95% quantiles of the variational distribution  $q_\lambda$  in parentheses. Panels A to D correspond to MCMC, Gaussian factor VA, mean field Gaussian VA and our proposed Hybrid VA, respectively.

Table A2: Estimate of  $V_\alpha$  for the tobit full data example using the Gaussian factor VA.

		B1			B2			B3			
		Intercept	Emails	Catal.	Paid S.	Emails	Catal.	Paid S.	Emails	Catal.	Paid S.
	Intercept	26.848 (26.51,27.2)	-	-	-	-	-	-	-	-	-
	Emails	-0.618 (-0.63,-0.61)	2.766 (2.7,2.84)	-	-	-	-	-	-	-	-
B1	Catal.	-0.025 (-0.03,-0.02)	0.016 (0.01,0.02)	0.584 (0.57,0.6)	-	-	-	-	-	-	-
	Paid S.	-0.129 (-0.15,-0.11)	0.082 (0.07,0.09)	0.003 (-0.01,0.01)	1.703 (1.68,1.73)	-	-	-	-	-	-
	Emails	0.633 (0.63,0.64)	-0.401 (-0.41,-0.39)	-0.016 (-0.02,-0.01)	-0.083 (-0.1,-0.07)	0.344 (0.34,0.35)	-	-	-	-	-
B2	Catal.	0.479 (0.47,0.49)	-0.303 (-0.31,-0.29)	-0.012 (-0.02,0)	-0.063 (-0.07,-0.05)	0.311 (0.3,0.32)	1.675 (1.64,1.71)	-	-	-	-
	Paid S.	0.097 (0.08,0.12)	-0.062 (-0.07,-0.05)	-0.003 (-0.01,0.01)	-0.013 (-0.02,0)	0.063 (0.05,0.08)	0.048 (0.04,0.06)	3.384 (3.29,3.49)	-	-	-
	Emails	0.753 (0.75,0.76)	-0.476 (-0.49,-0.47)	-0.019 (-0.03,-0.01)	-0.099 (-0.11,-0.08)	0.488 (0.48,0.5)	0.369 (0.36,0.38)	0.075 (0.06,0.09)	0.248 (0.24,0.25)	-	-
B3	Catal.	0.452 (0.44,0.46)	-0.286 (-0.3,-0.28)	-0.011 (-0.02,0)	-0.06 (-0.07,-0.05)	0.293 (0.28,0.3)	0.222 (0.21,0.23)	0.045 (0.03,0.06)	0.348 (0.34,0.36)	1.527 (1.5,1.55)	-
	Paid S.	0.016 (0,0.04)	-0.01 (-0.02,0)	0 (-0.01,0.01)	-0.002 (-0.01,0.01)	0.011 (0,0.02)	0.008 (0,0.02)	0.002 (-0.01,0.01)	0.013 (0,0.03)	0.007 (0,0.02)	2.749 (2.68,2.83)

The diagonal values are estimates of the variances of the random coefficients (i.e. the leading diagonal of  $V_\alpha$ ). The off-diagonal values are estimates of the correlations between the random coefficients (i.e. the correlations of the matrix  $V_\alpha$ ). The variational means are reported, along with the 95% quantiles of the variational distribution  $q_\lambda$  in parentheses.



Label	Brief description	Random Coefficients	
		Small E.g.	Full E.g.
Intercept	Scalar set to 1 for all observations	✓	✓
<i>Lagged Sales Variables</i>			
B1 past D sales	Total online sales of B1 in previous 4 weeks		
B2 past D sales	Total online sales of B2 in previous 4 weeks		
B3 past D sales	Total online sales of B3 in previous 4 weeks		
B1 past R sales	Total in-store sales of B1 in previous 4 weeks		
B2 past R sales	Total in-store sales of B2 in previous 4 weeks		
B3 past R sales	Total in-store sales of B3 in previous 4 weeks		
<i>Advertising Variables (in Adstock Form)</i>			
B1 Emails	Number of brand B1 ad emails received	✓	✓
B1 Catal.	Number of brand B1 ad catalogs received	✓	✓
B1 Paid S.	Number of brand B1 paid search click-throughs	✓	✓
B2 Emails	Number of brand B2 ad emails received		✓
B2 Catal.	Number of brand B2 ad catalogs received		✓
B2 Paid S.	Number of brand B2 paid search click-throughs		✓
B3 Emails	Number of brand B3 ad emails received		✓
B3 Catal.	Number of brand B3 ad catalogs received		✓
B3 Paid S.	Number of brand B3 paid search click-throughs		✓
<i>Variables included to control for endogeneity</i>			
Res Paid S.	Residuals from the paid search control function		
Organic S. CFs	No. clicks on organic search links for B1 ( $\log(\text{clicks} + 1)$ )		
Res Organic S.	Residuals from the organic search control function		
Res website V.	Residuals from the website visit control function		
Visits B1	Number of visits to B1 website ( $\log(\text{Visits} + 1)$ )		
<i>Other variables</i>			
log price	Log of B1 price index		
month1	January dummy variable		
month2	February dummy variable		
month3	March dummy variable		
month4	April dummy variable		
month5	May dummy variable		
month7	July dummy variable		
month8	August dummy variable		
month9	September dummy variable		
month10	October dummy variable		
month11	November dummy variable		
month12	December dummy variable		

Table A3: Brief description of the covariates in the mixed tobit model, with a full description given in Danaher et al. (2020). All covariates are included as fixed effects. Individual-level (zero mean) random coefficients are also considered for the intercept and advertising variables as indicated in last two columns for the small and full data examples, respectively. Advertising variables are entered in ‘AdStock’ form, which is exponentially smoothed with a short estimated lag.